

**CO₂ Capture in Chemically and Thermally Modified Activated
Carbons**

Carmem Natália de Pina Gonçalves

Final dissertation submitted to

Escola Superior Tecnologia e Gestão

Instituto Politécnico de Bragança

to obtain the Master's Degree in

Chemical Engineering

This work was carried out under the guidance of

Professor Dr. José António Correia Silva

and Professor Dr. Hélder Gomes

ACKNOWLEDGEMENTS

First, I want to thank God for guiding me in all my steps during my entire life and during my academic life.

To my family a big thanks to my mom and my sister Maria Augusta for your support during these years in every aspect, in the good moments but specially in the bad moments when I got bad results in some subjects. You have been there for me no matter what, to encourage me and my gratitude for you mom and sister is enormous just God knows how much I own you.

To all my brothers especially Augusto, José Manuel and Manuel Antonio and sisters Augusta, Ana Cristina, Maria Conceição, Neusa thank you for supporting me. To all my nephews specially Hérica Silvana. Thank you to my father Manuel Socorro.

To Irmã Teca, Manuel and Candida, without you this journey aren't possible am so glad and thankful to have you in my life.

To my supervisor José Antonio Correia Silva thank you for accepting to guide me during the realization of this dissertation and for that I am deeply thankful. To my co-supervisor Hélder Gomes for giving us the samples for the achievement of this work a very big thank you. And to all laboratory friends Adriano, Catarina, Hélder, José, Mehriban, Ivan, Sergio and Mohsen thank you so much. Pedro, I don't have words to thank you for all your support, am thankful.

To all my teachers that contributed for my academic formation.

To my dearest friends Magui, Rossana and Artur, I am grateful since I met you, even when we met in different circumstances, all I have do is to thank God for putting you in my path.

To my friends Denise, Diana, Henrich, Ivana, Lucas, Keven, Ameer, Hasmik, Siranush, Felismina, Jessica, Hassan, Sameen, Ogun, Teresa, Arminda, Treicy, Lourdes, Alven, Romana, Eduardo, Cristina, Durilde, Irina, my goddaughter Jercilene, my godson José and Ameray thank you for being there for me.

To my dearest friend Dicla I don't have words to explain what you mean for me, I think you are a mixture of friend and family and you know I don't need any word to tell you how important you are for me.

To my Portuguese friends Cesario, Liliana, Carlos and Amilcar. Cesario and Liliana you are my Portuguese best friends and I love you.

To Obete thank you for making me company in the library when I was writing this thesis while you were working on yours. And to all the people that contributed in one way or another to my growth.

ABSTRACT

In the pre-industrial era the great world powers were not preoccupied with the level of global warming since fossil fuels were not much explored. But the industrial revolution changed everything, as these energy sources started being used in the petrochemical industries as well as in metallurgical industries resulting in an increased worry concerning greenhouse gases.

Among the greenhouse gases, the carbon dioxide gas is one of the most common and impactful, as we are living in a world where the industrial development continues to grow and with that, it can be said that new technologies have been developed to reduce the greenhouse gases quantity in the atmosphere and consequently decrease global warming. Adsorption is one of those technologies and several adsorbent materials have been developed as well. To reach the objective of capturing the carbon dioxide a lot of studies have been made, to find an adsorbent with good adsorption capacity and that is easily accessible in economic terms.

Activated carbon as adsorbent is the perfect candidate for carbon dioxide capture by adsorption due to being economically viable and having a very significant surface area, as its superficial surface can be improved by means of chemical and thermal modifications. The 6 samples studied in this work were treated with: sulfuric acid (PACSA), nitric acid (PACNA), hydrogen peroxide (PACHP) and urea (PACNAU). And the thermal treatment used in the sample which was treated with urea occurred in a temperature range between 400-850 °C (PACNAUT). The ability of adsorbing carbon dioxide for each sample at different temperatures was measured. The best results were from the PACNAUT sample at temperatures of 40, 70 and 100 °C at 5 bar pressure where the adsorbed amount was 4,4537, 2,9805 e 2,1690 mmol g⁻¹ respectively. Which means, that the PACNAUT is the best sample.

RESUMO

Na era pré-industrial de um modo geral as grandes potências mundiais não tinham muito com que se preocupar a nível do aquecimento global, uma vez que as fontes de energias fósseis não eram muito exploradas. Mas com a revolução industrial tudo mudou, estas fontes de energias fósseis passaram a ser muito utilizados como por exemplo nas indústrias petroquímicas, as metalúrgicas etc., e com o aumento do uso dessas energias fósseis vem a preocupação da libertação dos gases causadores do efeito estufa.

Dentre esses gases está o dióxido de carbono que é um dos causadores do efeito estufa, vivemos num mundo onde a desenvolvimento industrial é bem evidente, e com isso pode se dizer que novas tecnologias foram estudadas para reduzir a quantidade dos gases causadores do efeito estufa da atmosfera e conseqüentemente reduzir o aquecimento global desenvolvendo várias técnicas para captura do dióxido de carbono como por exemplo a adsorção e vários materiais de adsorção também foram desenvolvidos. Para alcançar o objetivo de capturar o dióxido de carbono, vários estudos foram feitos para sua captura, ou seja, o estudo de um adsorvente que tenha uma boa capacidade de adsorção e que seja de fácil acesso em termos económico.

O carvão ativado como adsorvente é o candidato perfeito para captura de dióxido de carbono por adsorção por ser economicamente viável e por possuir uma área superficial important, uma vez que pode se melhorar a sua área superficial por modificação química e termal. As 6 amostras que foram estudadas neste trabalho tendo como amostra base o PAC onde 5 delas sofreram modificação químico onde foram utilizados: o ácido sulfúrico (PACSA), o ácido nítrico (PACNA), o peróxido de hidrogénio (PACHP) e a ureia (PACNAU). E o tratamento termal foi utilizado na amostra que foi tratado com ureia numa gama de temperatura entre de 400-850 °C (PACNAUT). A capacidade de adsorver o dióxido de carbono para cada uma das amostras para temperaturas diferentes. O melhor resultado obtido neste trabalho foi da amostra PACNAUT para gama de temperaturas entre 40, 70 e 100 °C e pressão de 5 bares onde a quantidade adsorvida foi de 4,4537, 2,9805 e 2,1690 mmol g⁻¹ respectivamente. O que torna o PACNAUT a melhor amostra de todas.

TABLE OF CONTENTS

List of figures	viii
List of tables	ix
Nomenclature	xi
1. INTRODUCTION	1
2. STATE OF ART	2
2.1. Global warming and CO ₂ capture	2
2.2. Physical Adsorption	3
2.3. Carbon dioxide chemistry	4
2.4. Adsorption Phenomena	5
2.5. Adsorption isotherm	7
2.5.1. Type I isotherm	8
2.5.2 Type II isotherms	9
2.5.3 Type III and Type V isotherms	9
2.5.4 Type IV isotherms.....	9
2.5.5 Type VI isotherms.....	9
2.6. Adsorbents	10
2.7. Pressure Swing Adsorption.....	11
3. EXPERIMENTAL SECTION	12
3.1. Material and Methods	12
3.1.1. Materials and Chemicals	12
3.1.2. Activation Techniques.....	12
3.1.3. Characterization of Activated Carbons	13
3.1. Breakthrough Experiments	14
3.2. Langmuir model.....	17
4. RESULTS AND DISCUSSIONS.....	19

4.1.	Breakthrough Curves	20
4.2.	Adsorption isotherms	22
4.3.	Comparison of different types of adsorbents for CO ₂ adsorption	27
5.	CONCLUSIONS	30
6.	BIBLIOGRAPHY	32
7.	APPENDIX	40
7.1.	Appendix A	40

List of figures

Figure 1. Concept and summary of CO ₂ capture and storage (CCS). Adapted from (Seul-Yi Lee et al., 2012).	3
Figure 2. Flow diagram of CO ₂ capture by adsorption. Adapted from (Yu et al., 2012). 6	
Figure 3. The IUPAC classification of isotherm. Adapted from (Guidance, 2011).	8
Figure 4. Schematic diagram of the experimental setup for the cyclic adsorption–desorption experiments: He, Helium bottle, CO ₂ , Carbon Dioxide bottle, Mass flow controller. Adapted from (Karimi et al., 2018).	16
Figure 6. PACNA Breakthrough curves at 313 K.	21
Figure 7. PACNA Breakthrough curves at 343 K.	21
Figure 8. PACNA Breakthrough curves at 373 K.	22
Figure 9. PAC equilibrium adsorption isotherm, fitted with Langmuir equation.	23
Figure 10. PACSA equilibrium adsorption isotherm, fitted with Langmuir equation. ...	23
Figure 11. PACNA equilibrium adsorption isotherm, fitted with Langmuir equation.	24
Figure 12. PACHP equilibrium adsorption isotherm, fitted with Langmuir equation. ...	24
Figure 13. PACNAU equilibrium adsorption isotherm, fitted with Langmuir equation. 25	
Figure 14. PACNAUT equilibrium adsorption isotherm, fitted with Langmuir equation. 25	

List of tables

Table 1. Physical properties of CO ₂	5
Table 2. Represents the distinction of physical adsorption and chemisorption.....	7
Table 3. The pore size according to IUPAC.....	14
Table 4. Elemental analyses of the AC materials.....	19
Table 5. Results of adsorption-desorption with N ₂ at 77K.....	21
Table 6. Total parameters and operational conditions used during the experiments.....	22
Table 7. Langmuir parameters at different temperatures.....	28
Table 8. Comparison of CO ₂ adsorption capacity in the different types of adsorbents...	31

Nomenclature

D_{micro}	average pore diameter (mm)
$F_{CO_2, in}$	molar flow rate of CO ₂ at the inlet of bed (ml/min)
$F_{CO_2, out}$	molar flow rate of CO ₂ at the outlet of bed (ml/min)
H	hydrogen
CO ₂	carbon dioxide
K_L	Langmuir adsorption constant (bar ⁻¹)
Kd_{∞}	affinity constant (bar ⁻¹)
M	molecular weight (g/mmol)
R _g	gas constant
$m_{adsorbent}$	mass of adsorbent in the bed (g)
N	nitrogen
P_b	pressure of bed at equilibrium (bar)
P_{CO_2}	partial pressure of CO ₂ (bar)
Q_e	adsorption capacity at equilibrium condition (mmol/g)
Q_m	maximum adsorption capacity (mmol/g)
R^2	regression determination coefficient (-)
S	sulfur
S_{BET}	specific surface area (m ² /g)
S_{EXT}	external surface area (m ² /g)
S_{micro}	microporous surface area (m ² /g)
t_b	breakthrough time (min)
t_s	saturation time (min)
T	temperature (K)
T_b	temperature of bed at equilibrium (K)

V_b	bed volume (cm^3)
V_d	dead volume (cm^3)
V_{mic}	micropore volume (mm^3/g)
V_{Total}	total pore volume (mm^3)
W_{mic}	width of micropore (nm)
$y_{\text{CO}_2, \text{feed}}$	molar fraction of CO_2 in feed stream (-)
Z	CO_2 compressibility factor at P_b and T_b (-)

Abbreviations

PAC	Powdered activated carbon
PACHP	Powdered activated carbons hydrogen peroxide
PACNA	Powdered activated carbon nitric acid
PACSA	Powdered activated carbon sulfuric acid
PACNAU	Powdered activated carbon nitric acid urea
PACNAUT	Powdered activated carbon nitric acid urea thermally
GHG	Greenhouse gases

Greek letters

α	sticking coefficient
ε	residual error (-)
ε_b	packed bed porosity (-)
ε_p	particle porosity (-)
ε_T	total porosity of bed (-)
ΔH	heat of adsorption (kJ/mol)

1. INTRODUCTION

Since the industrial revolution, we have noticed that the exploration of fossil fuels as energy source has been increasing. Over the years, the study of the impact of fossil fuels in the environment has been done and through those studies it was revealed that the main global warming problem is caused by those fossil fuels. Nowadays the concern about global warming is increasing, because the main source of energy used and that continues to be used to generate electricity besides renewable energy still is fossil fuels (coal, crude oil and natural gas). The continued consumptions of fossil fuels pollute the environment and accelerate global warming (Melikoglu, 2018).

When these fossil fuels are burning, they produce different types of gases that can drastically damage the environment by provoking temperature rise, greenhouse gases effect, high ocean level etc. Despite all those environmental damages, the major concerning issues among the global warming phenomenon are the greenhouse gases (GHG), including carbon dioxide (CO₂), methane (CH₄), chlorofluorocarbons (CFCs), and nitrous oxide (N₂O), and among these, CO₂ is the bigger threat to the environment. (Lee and Park, 2015).

Recent studies show that the energy consumption and global CO₂ emissions have increased by about 30% and consequently, an increase of temperature from 0.30 to 0.68 °C. Due this value many researches have been carried out in the field of CO₂ capture by adsorption process, especially as a post-combustion (PC) treatment of flue gas. One of the main approaches to decrease the amount of CO₂ in the atmosphere is Carbon Capture and Storage (CCS), which can reduce, control and optimize the overall mitigation costs by enhancing a great reduction in greenhouse gas (GHG) emissions. Separation of gases on a large scale is very important to industrial processes. For this purpose (gas separation) some processes were developed like absorption, cryogenic distillation, membrane separation. Among all these processes we shall take in account the adsorption process because it is the less expensive, faster and more efficient process (Karimi et al., 2018).

2. STATE OF ART

2.1. Global warming and CO₂ capture

Climate change has become one of the primary issues nowadays which has attracted much attention, observation, and investigation to find a solution for one of the most important environmental and energy policy issues in the 21st century (Karimi et al., 2014) (Nurrokhmah and Abu-zahra, 2013). One of the predominant greenhouse gases is carbon dioxide (CO₂) which it's sharply increasing in the atmosphere as well as its dangerous effects in the ecosystem, contributes to much environmental anxiety for researchers. (Continent et al., 2012) declared that the climate changes contribute to the enhancement of surface temperature of earth around 3-5 °C at end of this century and it causes ice and glacier melting which results in sea level increases of 95 cm and will disturb rainfall patterns (Hamdan et al., 2017). Based on reports, (Å and Peterson, 2007) combustion of coal, oil and natural gas industries including naphtha refineries (Karimi et al., 2015) and petro-chemical complexes (Iranshahi et al., 2014) are the source of more than 80% of CO₂ emissions in the world (Å and Peterson, 2007) and iron, steel and cement manufacturing are next (C. Zhao et al., 2012). Due to these industrial activities the CO₂ concentration has had a 70 ppm enhancement in the atmosphere from pre-industrial period until now (from 280 ppm to 400 ppm) while it's maximum amount should not pass 350 ppm (Wennersten et al., 2014). One of the main strategies to decrease the amount of CO₂ in the atmosphere is Carbon Capture and Storage (CCS) (Choi et al., 2009), which can reduce, control and optimize the overall mitigation costs by enhancing a great reduction in in greenhouse gas (GHG) emissions (Damiani et al., 2012)(Li and Fan, 2008). CCS is a group of technologies that have the ability of reduction emission from fixed industrial sources into the atmosphere, which based on the BLUE Map Scenario of the International Energy Agency (IEA), could contribute to a 19% reduction in CO₂ emissions, as most costly component of the CCS process, by 2050 (Figuroa et al., 2008) (Ie, 2006). The simple schematic of CCS has been presented in figure 1.

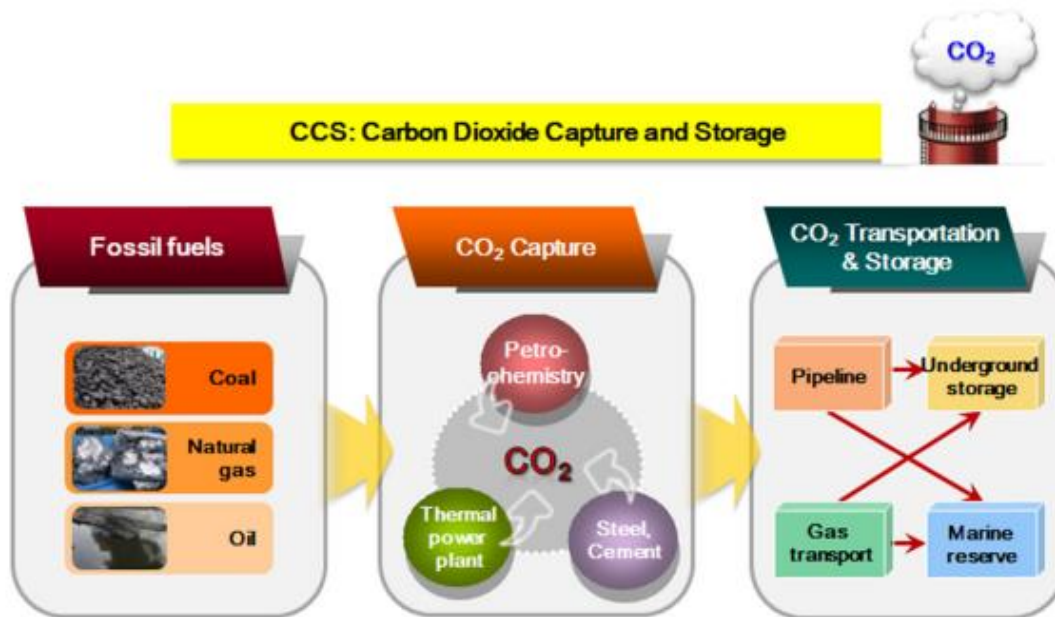


Figure 1. Concept and summary of CO₂ capture and storage (CCS). Adapted from (Seul-Yi Lee et al., 2012).

2.2. Physical Adsorption

Currently, adsorption with amine-based adsorbents is the most popular technology for CO₂ capture in the post-combustion processes throughout the world. In this method, the flue gas passes through an absorber tower and CO₂ reacts with amine solution, then this aqueous solution transports it to the absorber tower, whereby CO₂ is separated at higher temperature ($> 100\text{ }^{\circ}\text{C}$) (Ramdin, 2015)(Wang and Mitch, 2015). Besides its high performance this method has several main drawbacks, including: equipment corrosion, high energy consumption (for the solvent regeneration and solvent cost) as well as producing a wide range of hazardous substances both health and environmental aspects (McDonald et al., 2014)(McDonald et al., 2014). Thus, in the recent years, adsorption onto porous solids as an effective and versatile technique for the removal of different classes of pollutants from gaseous or liquid streams has received much attention.

The various physical adsorbents of CO₂ including porous carbons (A Arenillas et al., 2005)(Pevida et al., 2008), metal organic framework materials (Levan et al., 2009)(Bárcia et al., 2016), zeolite molecular sieves (Konduru et al., 2007)(Silva et al., 2014), lithium zirconate (Ochoa-ferna, 2006), silicon based mesoporous materials (Ochoa-ferna, 2006)(Hu and Liu, 2010) and other metal oxides materials (Yang and Lin, 2006) have been extensively developed in the recent years. Among these adsorbents, activated carbons are high attractive for CO₂ capture for several reasons. These materials are

amorphous porous forms of carbon that can be achieved in several ways. Agricultural residues, animal wastes, and liquid fractions obtained from the thermal treatments of plant wastes and coals (A and Ganvir, 2013)(Balsamo et al., 2013) are among the main sources of activated carbon as well as the pyrolysis of various carbon-containing resins, fly ash, or biomass are the other ones (Choi et al., 2009). Thus, the low cost and easy to handle of these materials in comparison with other ones, for example preparation and scale-up of MOFs (Metal Organic Frameworks), is one of the benefits of these materials. In addition, the hydrophobic character of activated carbons is their main benefits over zeolites and MOFs which results in a reduced effect of the presence of moisture that is a vital element for adsorbents in the post-combustion processes (Plaza et al., 2010). Furthermore, due to the weaker physical interaction of activated carbons with CO₂ and having a lower heat of adsorption compared with zeolites (13X) (Silva et al., 2012) and consequently less required energy for regeneration in the desorption process (Wahby et al., 2010) have made activated carbons a promising adsorbent for CO₂ capture.

2.3. Carbon dioxide chemistry

Carbon dioxide (CO₂) is a non-polar, colorless and odorless gas composed of a carbon atom double bonded to two oxygen atoms. CO₂ has sixteen bonding electrons in its valence shell. The C=O bonds are equivalent and short (1.16 °A), with a molecular diameter of 3.30 °A. Although both carbon-oxygen bonds are polar, the CO₂ molecule doesn't have a permanent electrical dipole due to its centrosymmetric structure. Once that two equal dipoles are located nearby, their total dipole moment is zero. Consequently, only two vibrational bands are detected in the IR spectrum: antisymmetric stretching mode at 2350 cm⁻¹ and a degenerate pair of bending modes at 667 cm⁻¹. However, CO₂ molecule has a strong quadrupole (-13.71×10^{-40} Coulomb/m²) as their positive charges overlap. This quadrupole interacts with the carbon lattice, allowing the gas molecule to enter the pores. Other flue gas component such as nitrogen, hydrogen, oxygen and methane have much smaller quadrupole moments which facilitate CO₂ interaction with walls inside activated carbon pores in competition with another component. The CO₂ physical properties are provided in table 1 (Shahkarami, 2017).

Table 1. Physical properties of CO₂.

Molecular Weight (g/mol)	44.01
Critical temperature (°C)	31,1
Critical pressure (bar)	73.9
Boiling point at 1.013 bar (°C)	-78.5
Specific volume STP (m ³ Kg ⁻¹)	0.506
Gas density STP (Kg/m ³)	1.976
Viscosity STP (μ.sm ⁻²)	13.72
pH of saturated CO ₂ solutions	3.7

2.4. Adsorption Phenomena

The real adsorption system can be defined as an equilibrium one including the adsorbent being in contact with the bulk phase and the so-called interfacial layer. This layer consists of two regions: the part of gas residing in the force field of the solid surface and the surface layer of the solid. The term ‘adsorption’ deals with the process in which molecules accumulate in the interfacial layer, but desorption denotes the reverse process (Do, 1998). In figure 2 is represented the flow diagram for CO₂ capture by adsorption.

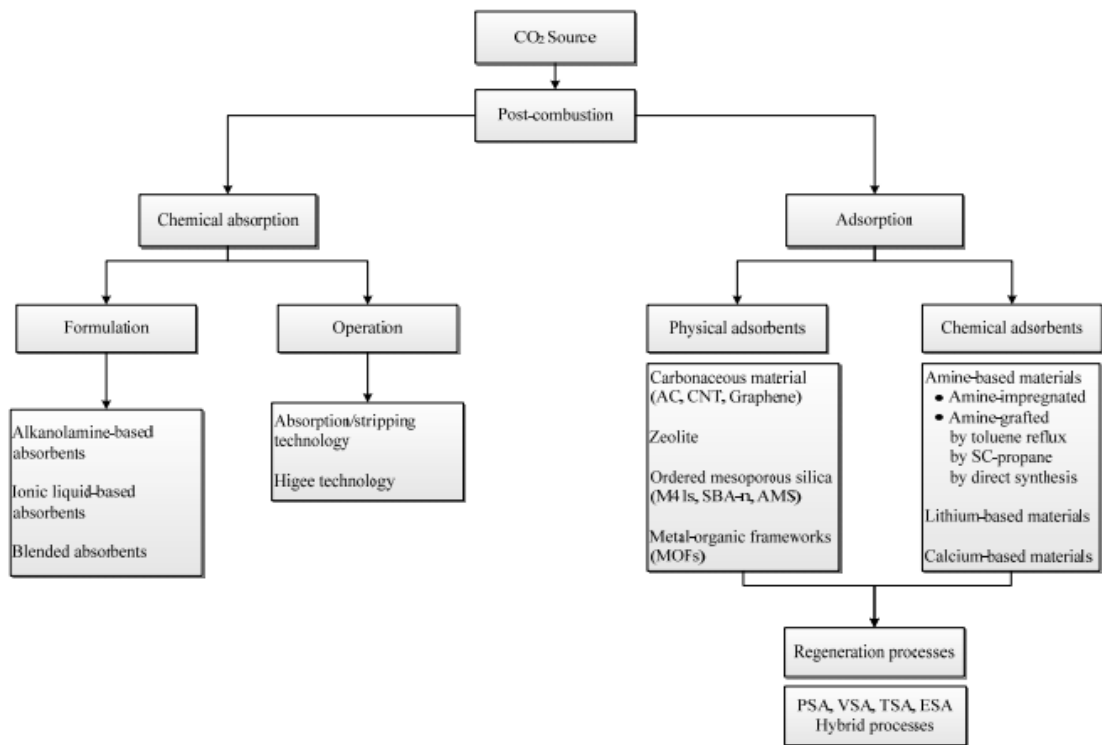


Figure 2. Flow diagram of CO₂ capture by adsorption. Adapted from (Yu et al., 2012).

In general, the phenomenon of adsorption can be classified in different ways. It can be classified as physical or chemical adsorption based on the scale of the heat of adsorption. Although such an approach is widely used because of its convenience, it is not very precise (Choi et al., 2001).

In a chemisorption there is a direct chemical bond between the adsorbate and the surface which means that, the surface shares electrons with the adsorbate molecule. The energy of chemisorption is of the same order of magnitude as the heat of reaction whereas energy ranges between 62-418 kJ/mol. Chemisorption is necessarily limited to a monolayer. Meanwhile in physical adsorption the adsorption happens mostly by van der Waals and electrostatic forces, the surface does not share electrons with the adsorbate and there is no chemical bond formed between the adsorbate and surface which is the reason that a physisorbed molecule usually keeps its identity and, on desorption, returns to its original form. Physical adsorption is exothermic, and the energy involved is not much larger than the energy of condensation of the adsorbate that ranges between 8-41 kJ/mol. Physical

adsorption generally arises for multilayers at relatively high pressures which depends on type of adsorbent and adsorbate used (Choi et al., 2001).

The general features which distinguishes Physical adsorption from chemisorption is shown in table 2 (M.Ruthven, 1984):

Table 2. Distinction between physical adsorption and chemisorption.

Physical Adsorption	Chemical Adsorption
Low heat of adsorption (<2 or 3 times latent heat of evaporation)	High heat of adsorption (>2 or 3 times latent heat of evaporation)
Non specific	Highly specific
Monolayer or multilayer	Monolayer only
No dissociation of adsorbed species	May involve dissociation
Only significant at relatively low temperatures.	Possible over a wide range of temperature
Rapid non-activated reversible	Activated, may be slow and irreversible
No electron transfer although polarization of sorbate may occur	Electron transfer leading to bond formation between sorbate and surface

2.5. Adsorption isotherm

The adsorption isotherm is a batch equilibrium procedure which provides data relating with the adsorbate adsorbed per unit weight of adsorbent with the amount of adsorbate remaining in the solution. The adsorption isotherm is used to determine the adsorption treatment feasibility (Gray et al., 1985). When an adsorbent meets the adsorbate (surrounding fluid) adsorption takes place. After a long time, the adsorbent and adsorbate reach equilibrium i.e. $W = f(P, T)$ where T is the temperature, P is the pressure and W is the equilibrium uptake of adsorbed adsorbate in unit of g/g or mol/g. If the temperature is kept constant, the change in equilibrium uptake against the pressure is called the

adsorption isotherm, $W = f(P)$. When the gas pressure is kept constant and the adsorbent temperature varies, the change in amount of adsorbate against the temperature is called the adsorption isobar, i.e. $W = f(T)$. Moreover, if the amount of adsorbate is kept constant, the change of pressure against the temperature is called the adsorption isosteric, i.e. $P = f(T)$. In an adsorption study, the adsorption isotherm is more likely to be used to express the result of adsorption rather than adsorption isobar or isosteric. For the designing of any adsorption, process equilibrium isotherm is one of the more important parameters. The amount of adsorbent needed in the absorber is determined by the equilibrium data, which in turn determines the key dimension and operation time for the process.

The adsorption isotherm can have different shapes, which is based on the adsorbent, adsorbate and the adsorbent-adsorbate interaction. Figure 3 shows the classification of six types of adsorption isotherm according to IUPAC (International Union of Pure and Applied Chemistry).

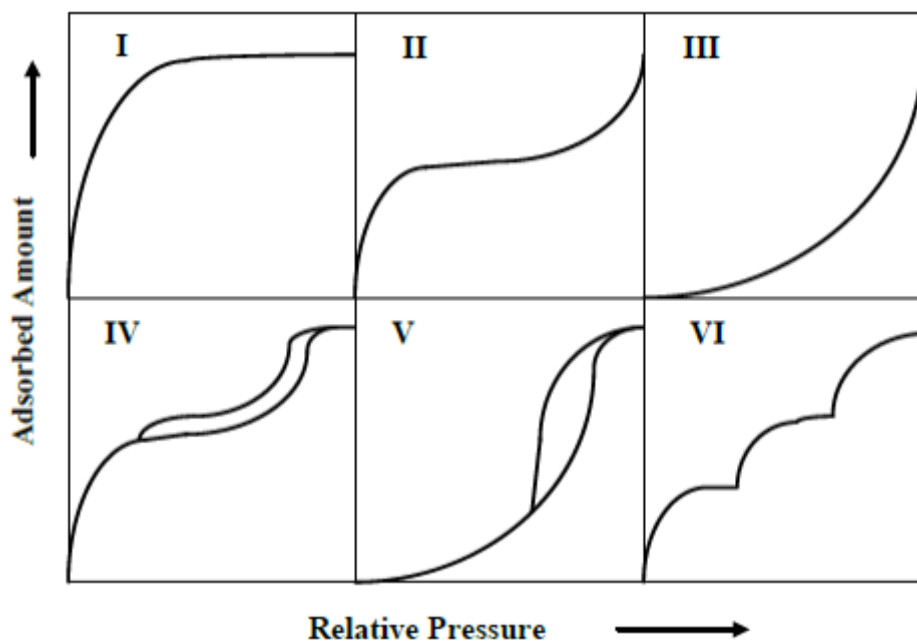


Figure 3. The IUPAC classification of isotherm. Adapted from (Guidance, 2011).

2.5.1. Type I isotherm

When an adsorbent contains very fine micropores where the pore dimension is only a few molecular diameters, the potential field of force from the neighboring walls of the pores

will overlap causing an increase in the interaction energy between the adsorbent surface and gas molecules.

2.5.2 Type II isotherms

These isotherms correspond to multilayer physical adsorption. It is concave at low relative pressure, and then linear for a small pressure range where monolayer coverage is complete, and subsequently become convex to the relative pressure axis, indicating the formation of multilayer whose thickness increases progressively with an increase in relative pressure.

2.5.3 Type III and Type V isotherms

Type III and Type V isotherms are characterized by being convex to the relative pressure axis. In type III isotherms the convexity continues throughout the isotherm but in type V the isotherm reaches a plateau at high relative pressure. The convexity of the isotherm is the indication of cooperative adsorption, which means that the already adsorbed molecules tend to enhance the adsorption of other molecules. In other words, we can say that it supports the adsorbate-adsorbate interaction.

Type III isotherms are generally observed in the case of nonporous or highly microporous adsorbents, and type V on mesoporous or microporous adsorbents for the adsorption of both polar and non-polar adsorbates.

2.5.4 Type IV isotherms.

Type IV isotherms are obtained for adsorbent containing pores in the mesopore range. The shape of the type IV isotherm follows the same path as type II at lower relative pressure and the slope start decreasing at higher pressure. At saturation vapor pressure the isotherm levels, off to constant value of adsorption. The portion of isotherm, which is parallel to the pressure axis, is attributed to pore filling by capillary condensation.

2.5.5 Type VI isotherms.

Type VI isotherms show discrete steps which may be caused by multilayer formation in different ranges of micropores (Guidance, 2011).

2.6. Adsorbents

The porous solid of a given adsorption process is a critical variable. The success or failure of the process depends on how the solid performs in both equilibria and kinetics. A solid with good capacity but slow kinetics is not a good choice as it takes adsorbate molecules too long time to reach the particle interior. This means that the gas spends a long time inside of the column, hence a low throughput. Still, a solid with fast kinetics but low capacity is not good either as a large amount of solid is required for a given throughput. Thus, a good solid is the one that provides good adsorptive capacity as well as good kinetics. To satisfy these two requirements, the following aspects must be satisfied: (1) the solid must have reasonably high surface area or micropore volume and (2) the solid must have relatively large pore network for the transport of molecules to the interior (Do, 1998).

During past few years, several researches about different types of adsorbents for CO₂ capture have been made. According to (Choi et al., 2009) the three most important physical adsorbents are carbonaceous materials (activated carbon), inorganic porous materials (zeolites) and MOFs adsorbents. These adsorbents have adsorption characteristic that allow them to be different from each other, for example, the activated carbons have high surface area, high amenability to pore structure modification and surface functionalization plus they can be regenerated easily and owing to their low cost. The zeolites adsorption capacity can be affected by their size, charge density and chemical composition of cations in their porous structure (Wang et al., 2011). Regards to MOFs, according to (Li et al., 2011) it may be noted that high surface area, controllable pore structures and tunable pore surface properties, can be easily tuned by changing either the metallic clusters or the organic ligands. Among these characteristics the major drawbacks of these adsorbents (zeolites and MOFs) are the affinity that they have with water, which drastically reduce their adsorption capacity and requires a high regeneration temperature (usually above 300°C) and this will become expensive because of the high energy requirement. The activated carbon has a hydrophobic character. The pore size according to IUPAC is shown in table 3.

Table 3. The pore size according to IUPAC

Type	Pore size (nm)
Supermicro-pore	0.7-2
Micro-pore	<2
Meso-pore	2-50
Macro-pore	>50

2.7. Pressure Swing Adsorption

Nowadays many researches of capturing CO₂ for carbon sink as a greenhouse mitigation have been published. To recover CO₂ from flue gas produced by power plants, steel mills, and cement kilns, the gas absorption technology can be used with carbonates or alkanolamines solvents. Although in a conventional MEA (Monoethanolamine) absorption processes there is a major disadvantage since the regeneration of the solvent is highly energy intensive (Audus, 1997; Meisen and Shuai, 1997). Also, the absorption process is expensive and involves corrosion problems.

For that its crucial to find solutions that allow improvement of technologies for CO₂ capture that are needed to reach low energy penalties, in addition as alternative technologies pressure swing adsorption (PSA) could be applicable for removal of CO₂ from flue gas streams. As it is a simple process to operate, the PSA systems have an advantage over absorption or cryogenic systems, PSA necessitates only a few vessels capable of withstanding pressure changes. The PSA and absorption systems have one thing in common is that both can do the regeneration of adsorbent that can be reused but PSA system has no limitation compared to other technologies like absorption which is technical experience in the matter of CO₂ recovery from industrial streams such as post combustion flue gas (Ho et al., 2008). In respect to CO₂ capture by adsorption process, the most used technology in industrial scale is Pressure Swing Adsorption.

Due its cyclic adsorption process, PSA allows for a continuous separation of gas streams. However, its performance works by periodic changes of pressure, aiming for the

optimization of contaminants removal. The main way to know how the PSA system acts is by measuring the product purity and recovery (Chung et al., 1998).

3. EXPERIMENTAL SECTION

In this work, six samples were analyzed, where one of these samples generated the others 5 activated carbon samples through chemical and thermal treatment. In this section the breakthrough curves experiments will be discussed, how the activated carbon was treated, its performance and the studies of the isotherm curves.

3.1. Material and Methods

3.1.1. Materials and Chemicals

PAC (powder activated carbon) is an extruded carbon material produced by steam activation. The commercial powder activated carbon Norit ROX 0.8 (PAC) with high purity (ash content of only 3 wt.%) was supplied in cylindrical pellets (diameter and average length were 0.8 mm and 4.0 mm, respectively). Urea (65 wt.%), nitric acid (65 wt.%) and sulphuric acid (96–98 wt.%) were supplied by Riedel–de-Haën, and hydrogen peroxide (30%, w/v) was obtained from Panreac. In addition, the used gases, carbon dioxide and helium with purity of 99.98% and 99.95% respectively were supplied by Air Liquide.

3.1.2. Activation Techniques

Physically (thermally) and chemically methods are the two main techniques for synthesis of activated carbon (AC). In the thermal activation, the materials are carbonized in the temperature range of 400-850 °C, while in the chemical method activation takes place by

heating the mixture of precursor and dehydrating agent or oxidant (Rodríguez-Reinoso, 2002).

The original PAC (Norit ROX 0.8) was grinded and sieved to the particle sizes ranging from 0.106 to 0.250 mm, then, was chemically modified by liquid phase, thermal and hydrothermal. In this way, three samples were prepared by treating 25 g of the original PAC with 500 mL of 30 % (w/v) H₂O₂ (PACHP sample), 18 M of H₂SO₄ (PACSA sample) and 5 M of HNO₃ (PACNA sample) at the room temperature (24 h), 150 °C (3h) and 110 °C (3 h), respectively. After these treatments, all samples were filtered and washed several times with distillate water until the neutrality of the ringing water is reached. Later, samples were dried at 110 °C in an oven, during 18 h, resulting in the PACHP, PACSA and PACNA materials. Other two samples were obtained in the successive treatments of the PACNA material. First one was obtained through the treatment of PACNA with 1 M of urea solution (50 mL per 2 g of PACNA) at 200 °C for 2h, under its own vapour pressure in a stainless-steel high-pressure batch reactor. Later, the material was filtered, washed and dried at the same conditions which resulted in PACNAU material. Second sample was obtained from a gas phase thermal treatment of 1 g of the PACNAU sample under N₂ flow (100 cm³•min⁻¹) at 120 °C, 400 °C and 600 °C for 1 h at each temperature and then at 800 °C during 4 h, resulting in the PACNAUT materials.

3.1.3. Characterization of Activated Carbons

Textural characterizations of the activated carbons were obtained from N₂ adsorption–desorption isotherms at -169 °C, using a Quanta-chrome NOVA 4200e adsorption analyzer. BET method, (Brunauer et al., 1938) was used to determinate the specific surface area (S_{BET}) of activated carbons and *t*-method (employing ASTM standard D-

6556-01 for the thickness calculation) to determinate the external surface area (S_{ext}) and the micropore volume (V_{microp}) (de Boer et al., 1965)

Subtracting the S_{ext} from S_{BET} resulted in the microporous surface area (S_{microp}), then the average pore diameter (D_{microp}) was determined by approximation ($D_{microp} = 4 V_{microp}/S_{microp}$). The total pore volume (V_{Total}) was calculated at $p/p^0 = 0.98$. In addition, microporosity was evaluated by employing the empiric micropore analysis method of (Mikhail et al., 1968). (MP) and theoretical Horvath-Kawazoe (HK) method (Horvath and Kawazoe, 1983) and mesoporosity was assessed by using Barrett-Joyner-Halenda method, (BJH) applied for N_2 adsorption and desorption ($p/p^0 > 0.35$) (Barrett et al., 1951).

Calculations of those methods were all done by using Nova Win software v11.02. Elemental compositions (C, H, N and S) were quantified by employing a Carlo Erba EA 1108 Elemental Analyzer. In the table 4 are expressed the results of elemental analyses.

Table 4. Elemental analyses of the AC materials.

	C (%)	H (%)	S (%)	N (%)	Remaining (%)
PAC	79.0	1.4	0.6	0.0	19
PACSA	76.1	1.7	1.1	0.0	21.1
PACHP	81.3	1.3	0.6	0.0	16.8
PACNA	70.5	2.3	0.4	1.4	25.5
PACNAU	75.3	2.6	0.3	3.2	18.6
PACNAUT	88.5	2.1	0.4	2.7	6.3

3.1. Breakthrough Experiments

For the realization of the breakthrough experiments all the gases (He and CO_2) were supplied by *Air Liquide* (France) with high level of purity: helium ALPHAGAZ 2 (99,9998%), carbon dioxide N48 (99,995%).

The Adsorption process took place in a gas chromatograph, SRI 310C (*SRI Instruments*, Torrance, United State of America), equipped with a thermal conductivity detector (TCD) where He was used as the carrier gas as is showed in figure 4.

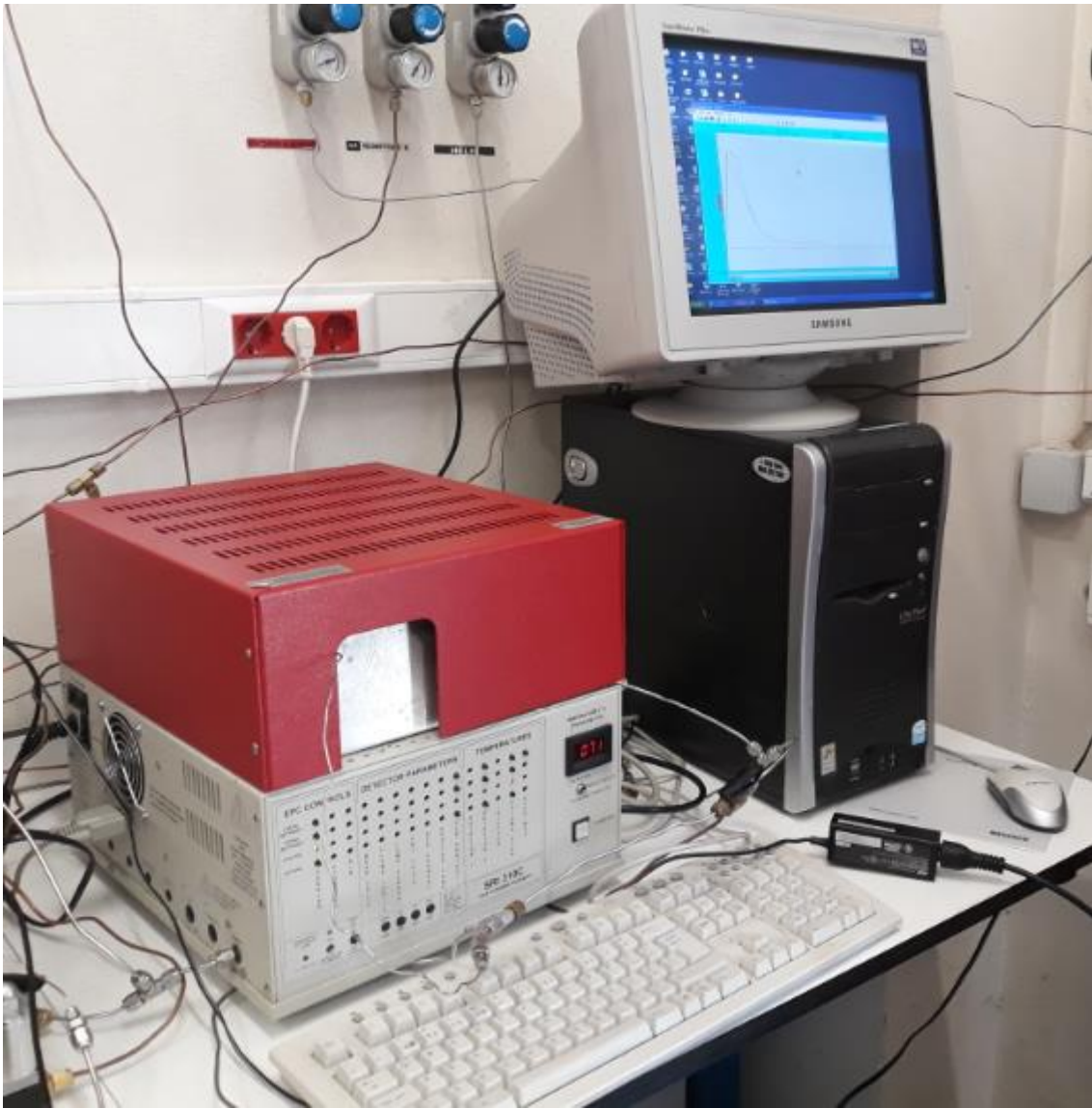


Figure 4. The gas chromatograph SRI 310C connected to the computer.

The gas chromatograph has an oven with a programmable temperature from room temperature up to 220° C, unlimited ramps and it has also a faster cooling. The data acquisition system, *peak simple*, is too easier to make connection with the computer.

To estimate the performance of the studied adsorbents, the CO₂ saturation (i.e., equilibrium) adsorption capacities of the activated carbon, the breakthrough measurements for the CO₂ containing binary gas mixture were conducted in a fixed-bed adsorption unit (Fig. 5).

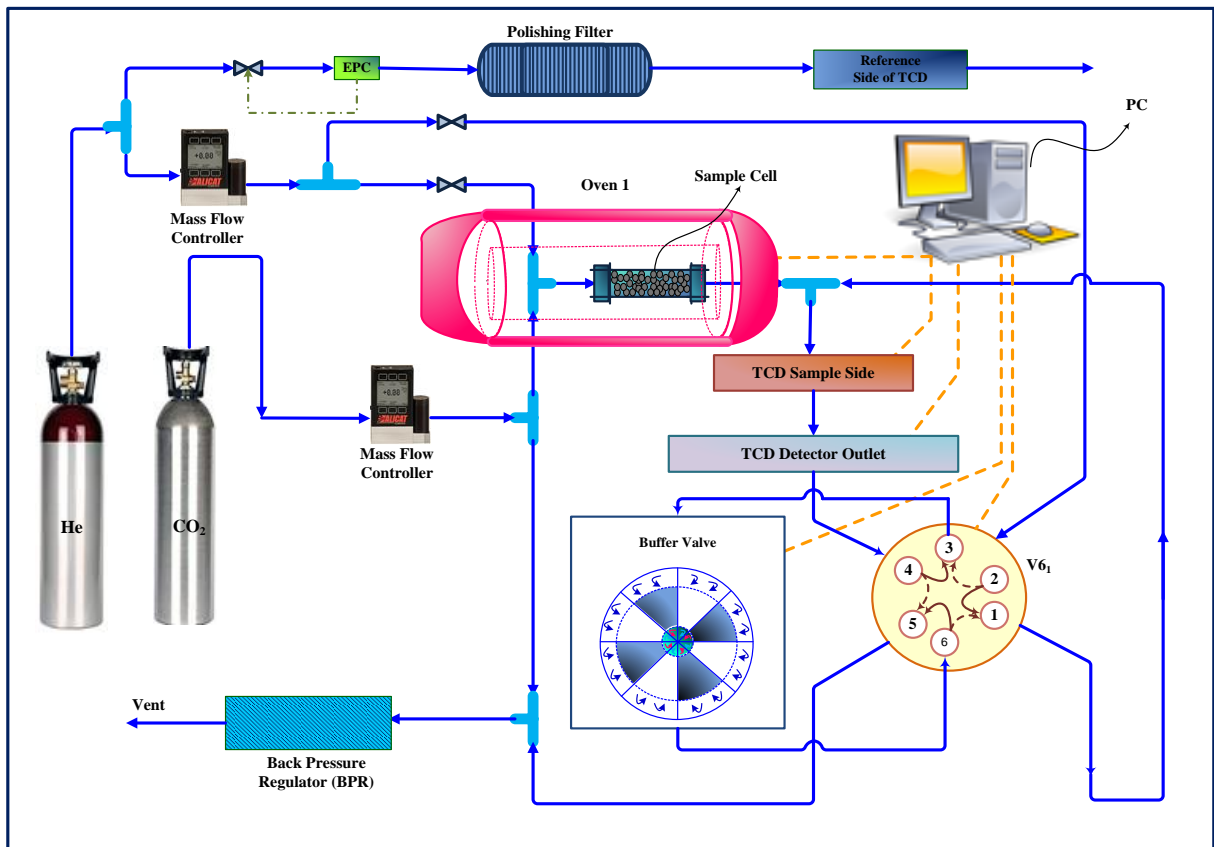


Figure 5. Schematic diagram of the experimental setup for the cyclic adsorption–desorption experiments: He, Helium bottle, CO₂, Carbon Dioxide bottle, Mass flow controller. Adapted from (Karimi et al., 2018).

The stainless-steel fixed bed reactor has a 10 cm height with inner diameter of 0,46 cm and 0,089 cm of wall thickness. The gas system consists in 3 lines fitted with two Mass Flow Controller (MFC), model GFC17 from AALBORG, New York, United State of America (one mass flow controller for helium and another one for carbon dioxide), the first line is for the helium feed and the second one is for the mixture gas feed (carrier gas and CO₂) and the third one is for feed of the binary gas mixture.

The column was packed with the activated carbons to ensure the measurement of adsorption amount of CO₂ during the experiments, once the column is filled, the gas that should pass first through the column should always be the carrier gas. Before the experiments are started, it is necessary to feed the packed column with He during 12 hours at 463K, the He flow rate is measured and CO₂ flow rate as well before recording the flow rate of He and CO₂. Once the experiment is started the line with He and the line with gas mixture goes to one switch valve that allows which desired line should pass through the adsorption column. The not desired line is redirected to line 3. All the system pressure is

controlled by a Back- Pressure-Regulator 5 bar model from *Alicat Scientific*, Tucson, United States of America.

When the line with gas leaves the column, it goes through the TCD that can detect the concentration of all gas around 100 ppm, also this signal helps to know the correct breakthrough time that the adsorbate (CO₂) leaves the adsorption column. To obtain the CO₂ adsorption capacity the follow breakthrough curves equation was used. In gas phase adsorption, the adsorbed gas quantity in the column empty spaces, can be disregarded regarding the quantity adsorbed by the adsorbent bed.

$$Q_{CO_2} = \frac{I}{m_{adsorbent}} \left[\int_0^{t_s} (F_{CO_2, in} - F_{CO_2, out}) dt - \frac{y_{CO_2, feed} P_b \varepsilon_T V_b}{ZR_g T_b} - \frac{y_{CO_2, feed} P_b V_d}{ZR_g T_b} \right] \quad (1)$$

$$\Leftrightarrow Q_{CO_2} = \frac{1}{m_{adsorbent}} \int_0^{t_s} (F_{CO_2, in} - F_{CO_2, out}) dt$$

The t_s means the saturation time of the bed and ε_T is the total porosity of bed. ε_T is calculated by the following equation:

$$\varepsilon_T = \varepsilon_b + (1 - \varepsilon_b) \varepsilon_p \quad (2)$$

Breakthrough tests were performed in constantly adsorption–desorption cycles where the adsorbent reached saturation (maximum adsorption capacity of the adsorbed component) through the adsorption step although it was completely regenerated during the desorption step where the inert gas (He) was used to clean the sample after every adsorption step.

3.2. Langmuir model

To better understand the adsorption process, several thermodynamic models were developed, and the Langmuir model is one of them due to its theoretical simplicity to describe the monolayer adsorption onto homogeneous surface (Ammendola et al., 2017).

According to (Vieira et al., 2018) the Langmuir model is an equation originally deduced for adsorption of gas molecules in solid surfaces. The Langmuir isotherm is based on the following assumptions (Pérez-Marín et al., 2007):

- adsorbed molecule is chemically adsorbed at a fixed number of well-defined sites,
- each site can only hold one adsorbed molecule,
- all sites are energetically equivalent,
- and there is no interaction between the molecules adsorbed.

The Langmuir model is usually used to fit experimental data. Based on this, the following mathematical equation of the Langmuir model is normally applied (Clarke and Irving Langmuir, 1916):

$$Q_e = \frac{Q_m K_L P_{CO_2}}{1 + K_L P_{CO_2}} \quad (3)$$

where Q_m (mmol g⁻¹) is the maximum monolayer adsorption capacity of the adsorbent, P_{CO_2} (bar) is the equilibrium partial pressure of the gas adsorbed, with K_L (bar⁻¹) is the Langmuir adsorption constant or the affinity constant. It is a measure of how strong an adsorbate molecule is attracted to a surface. When K_L is larger, the surface is covered with more adsorbate molecule because of the stronger affinity of the adsorbate molecule towards the surface.

$$K_L = \frac{\alpha \exp\left(\frac{\Delta H}{R_g T}\right)}{k_{d\infty} \sqrt{2 \pi M R_g T}} = K_\infty \exp\left(\frac{\Delta H}{R_g T}\right) \quad (4)$$

$$K_\infty = \frac{\alpha}{k_{d\infty} \sqrt{2 \pi M R_g T}} \quad (5)$$

ΔH is the heat of adsorption, α is the sticking coefficient, T is the temperature, R_g is the gas constant and M is the molecular weight. The validity of the achieved model is

evaluated by the correlation determination coefficient (R^2), which its scale is [0-1] and for the best fitting it should be closer to the unity.

4. RESULTS AND DISCUSSIONS

The powder activated carbon (PAC) served as a base for the followed activated carbons: PACHP, PACNA, PACNAU, PACSA and PACNAT. These activated carbons were modified chemically and thermally. The chemical treatments modifiers agents used were; H_2SO_4 (PACSA sample), nitric acid (PACNA), H_2O_2 (PACHP sample) and urea (PACNAU). The thermal treatment was carried out under a temperature range between 400-850 °C (PACNAUT). The results for the adsorption-desorption process are presented in table 5.

Table 5. Results of adsorption-desorption with N_2 at 77K.

	S_{BET} ($m^2 \cdot g^{-1}$)	S_{ext} ($m^2 \cdot g^{-1}$)	S_{mic} ($m^2 \cdot g^{-1}$)	V_{mic} ($mm^3 \cdot g^{-1}$)	V_{mic}/V_{Total} (%)	W_{mic} (nm)
PAC	885 ± 10	160 ± 2	725 ± 12	314 ± 1	58	1.73 ± 0.03
PACSA	862 ± 9	150 ± 2	712 ± 11	308 ± 1	59	1.72 ± 0.03
PACHP	893 ± 10	159 ± 2	734 ± 12	319 ± 1	58	1.73 ± 0.03
PACNA	889 ± 10	170 ± 2	719 ± 12	311 ± 1	57	1.72 ± 0.03
PACNAU	960 ± 11	181 ± 2	778 ± 12	336 ± 1	58	1.72 ± 0.03
PACNAUT	1055 ± 11	197 ± 2	858 ± 12	367 ± 1	58	1.71 ± 0.03

As mentioned before, the surface area is the main feature for a high adsorption quantity and according to the values from surface area showed in table 5 it can be observed that when the PAC is treated with H_2SO_4 the S_{BET} area can be lower than PAC before treated. For the PACNA and PACHP samples their S_{BET} differ a little bit from the original sample (PAC). Therefore, the only samples with significant S_{BET} are those who had urea and thermal treatment, (PACNAU and PANAUT).

To perform the CO_2 capture by adsorption the following table shows the used values for adsorbents mass, the helium and the carbon dioxide flow rates and operational conditions. It should be noted that according to the data from table 6 the same flow rates were used and more unless the same mass for all samples.

Although for this process, each sample was used five times for each temperature of 313, 343, 373 K, and the total pressure range between 1 bar to 5 bar.

Table 6. Total parameters and operation conditions used during the experiments.

	PAC	PACSA	PACHP	PACNA	PACNAU	PACNAUT
Mass of sample (gr)	~0.6	~0.6	~0.6	~0.6	~0.6	~0.6
Ambient pressure (bar)	1	1	1	1	1	1
Ambient temperature (k)	293.75	295.55	294.85	295.25	293.05	294.35
CO ₂ flow rate (ml/min)	~10	~10	~10	~10	~10	~10
Helium flow rate (ml/min)	~9	~9	~9	~9	~9	~9
Particle sizes (µm)	106-250	106-250	106-250	106-250	106-250	106-250
Porosity (total volume porous, mm ³ .g ⁻¹)	541	520	545	547	581	635
Operating Conditions						
	PAC	PACSA	PACHP	PACNA	PACNAU	PACNAUT
Temperature (K)	313, 343, 373	313, 343, 373	313, 343, 373	313, 343, 373	313, 343, 373	313, 343, 373
Total Pressure (bar)	1,2,3,4,5	1,2,3,4,5	1,2,3,4,5	1,2,3,4,5	1,2,3,4,5	1,2,3,4,5

4.1. Breakthrough Curves

To obtain the breakthrough curves it was necessary to record the dynamic behaviour by a continued registration of the CO₂ flow rate at the column outlet as a function of time. To know the dynamics estimation of the column it must be considered the adsorption capacity and the time that the adsorbent reaches the saturation.

The CO₂ adsorption capacity (Q_{CO_2}) was calculated by numerical integration of the breakthrough curve data by Eqn (1). For example, all breakthrough curves obtained for the activated carbon PACNA at the same CO₂ flow rate, total partial pressure and temperatures (313 K, 343 K and 373 K) are illustrated in figure 6,7 and 8.

The curves show that initially the CO₂ can be efficiently adsorbed on activated carbon. It can be observed at higher adsorption temperature corresponds to low breakthrough time. The CO₂ adsorption time for PACNA at a total pressure of 5 bars is about 5,20 min, 3,35 min, and 2,48 min at adsorption temperature of 313 K, 343 K and 373 K respectively. The steep nature of these curves is indicative of an efficient use of the adsorbent in the dynamic process.

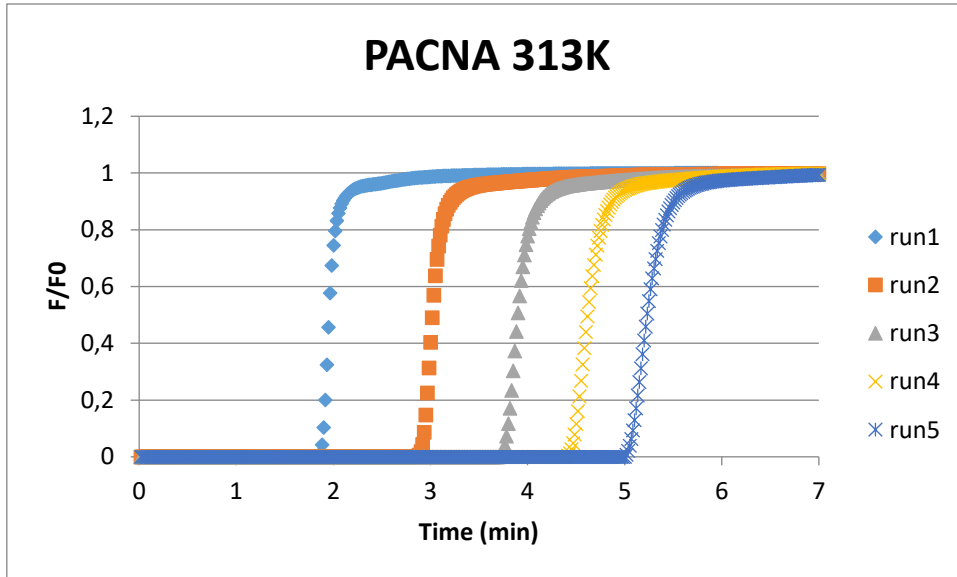


Figure 6. PACNA Breakthrough curves at 313 K.

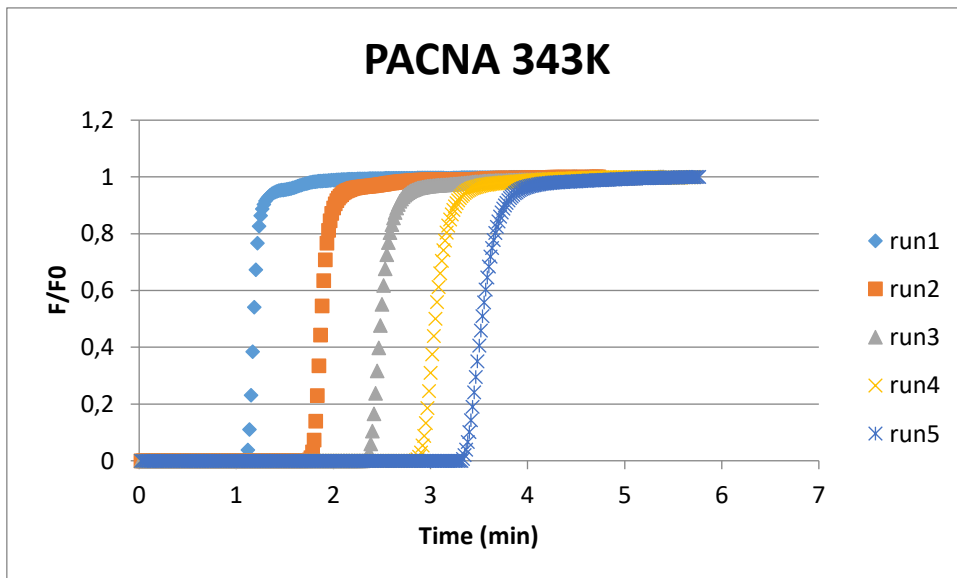


Figure 7. PACNA Breakthrough curves at 343 K.

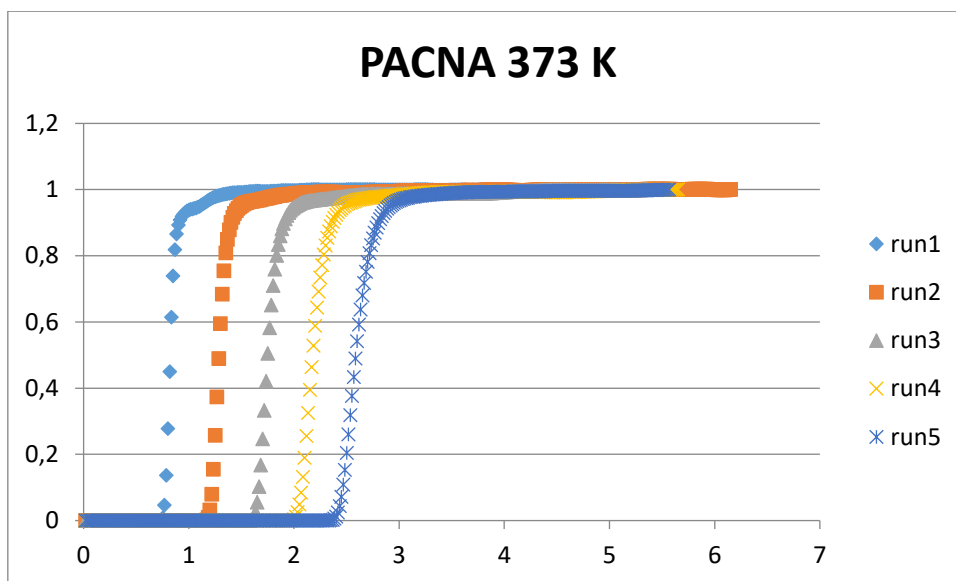


Figure 8. PACNA Breakthrough curves at 373 K.

4.2. Adsorption isotherms

The isotherms adsorption was measured at temperature range between 313, 343 and 373 K and pressure range between 1 to 5 bar.

The breakthrough curves obtained are of crucial importance, because through these breakthrough curves calculations it will be possible to determine the isotherms of adsorption. According to (Singh and Kumar, 2017) it is noted that through the adsorption isotherms a better idea of the adsorbate-adsorbent pairs adsorption behaviour and performance can be obtained.

The experimental data of CO₂ adsorption was fitted with the Langmuir model. The figures 9 to 14 bellow represent the experimental CO₂ isotherms at different temperatures and fitted with the Langmuir model for PAC, PACHP, PACSA, PACNA, PACNAU and PACNAUT. The adsorbed material quantity is showed in terms of mmol of pure component adsorbed by grams of adsorbent. The landmarks points are the experimental data while the solid lines represent the isotherm model used in this study.

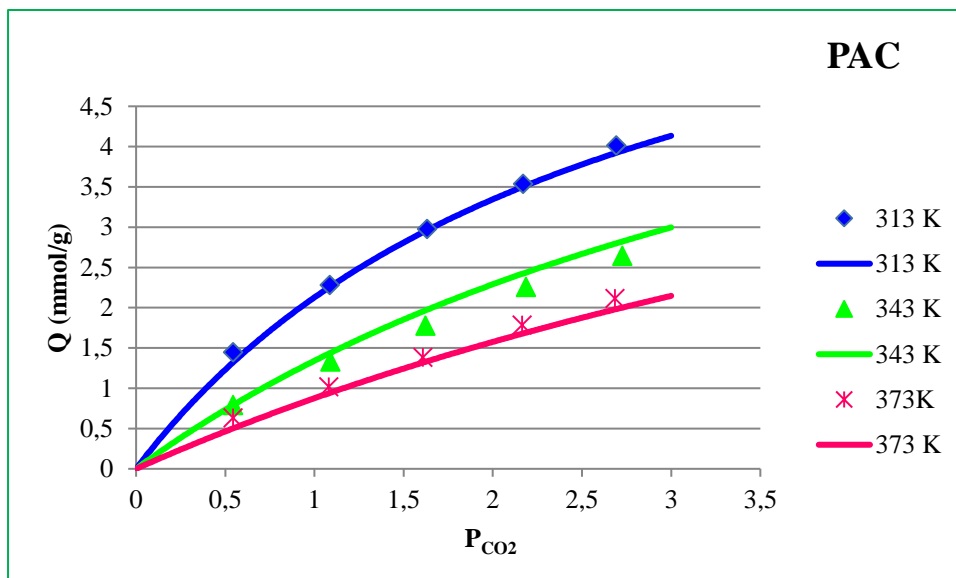


Figure 9. PAC equilibrium adsorption isotherms fitted with Langmuir equation.

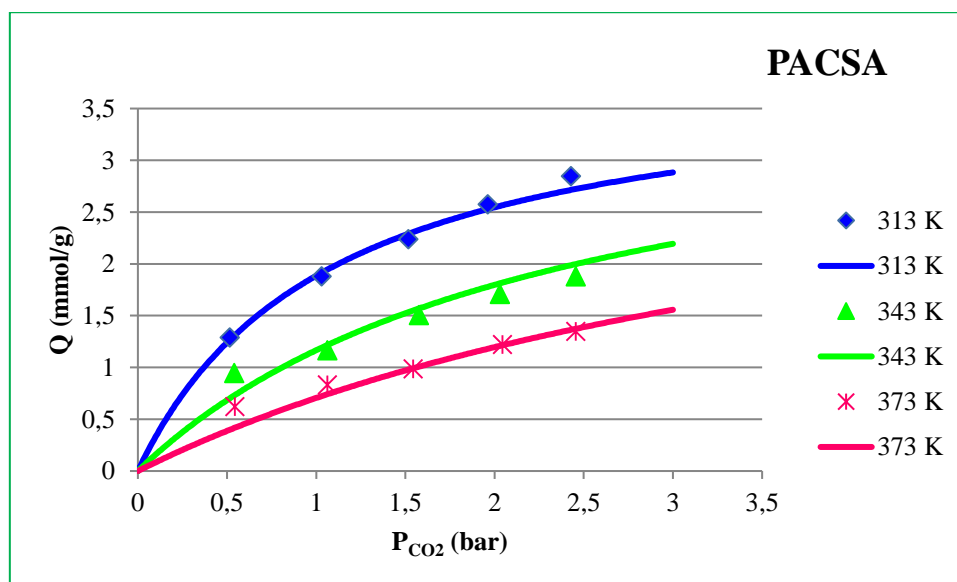


Figure 10. PACSA equilibrium adsorption isotherms fitted with Langmuir equation.

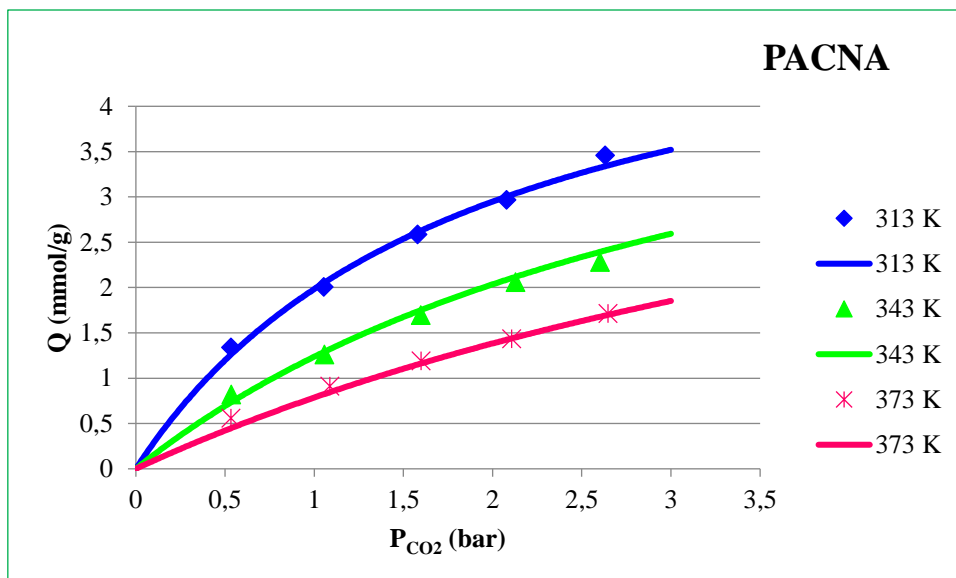


Figure 11. PACNA equilibrium adsorption isotherms fitted with Langmuir equation.

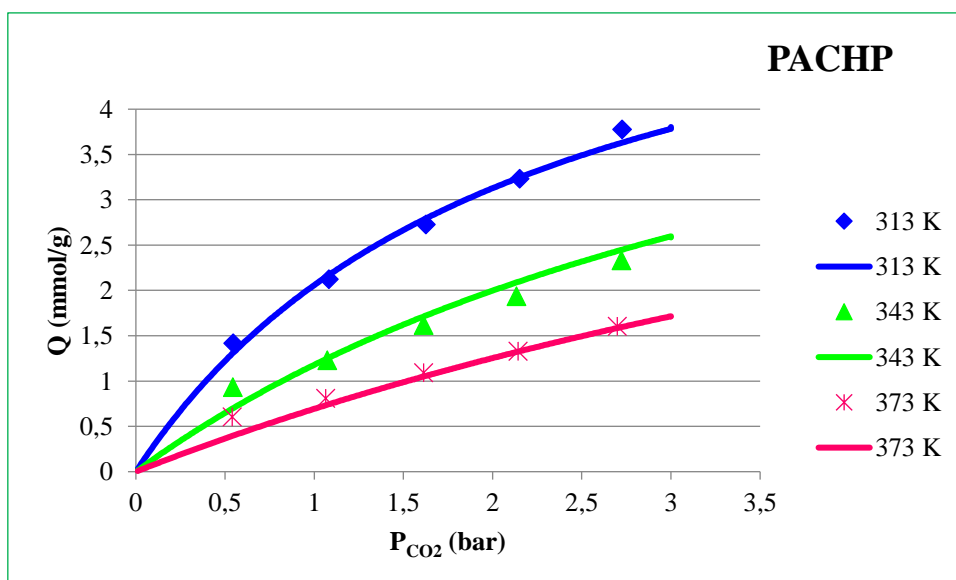


Figure 12. PACHP equilibrium adsorption isotherms fitted with Langmuir equation.

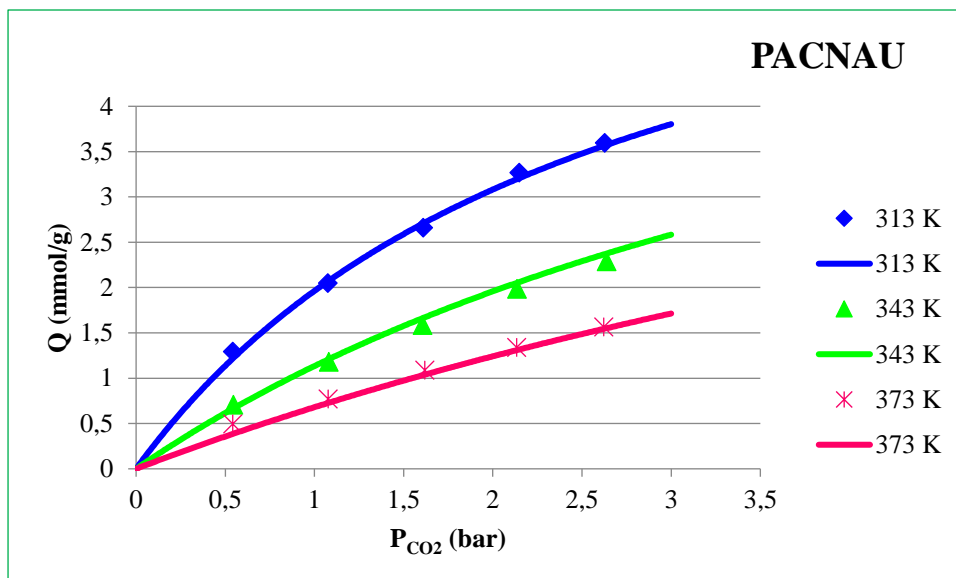


Figure 13. PACNAU equilibrium adsorption isotherms fitted with Langmuir equation.

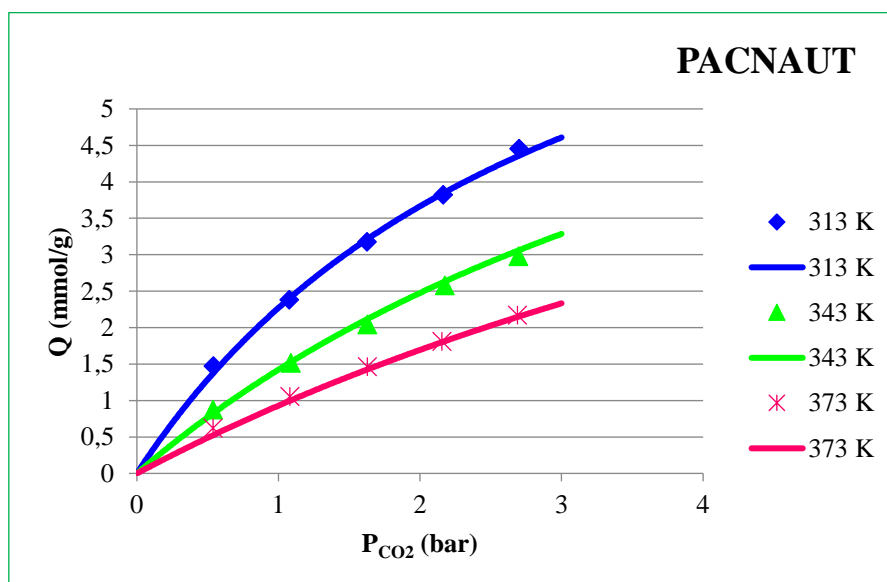


Figure 14. PACNAUT equilibrium adsorption isotherms fitted with Langmuir equation.

From the figures mentioned above it can be observed that when the temperature increases, the quantity of CO₂ adsorbed decreases, that happen due to the strength of the binding forces between the adsorbate and adsorbent in agreement with the exothermic nature of adsorption (Singh and Anil Kumar, 2016). According to (Rashidi et al., 2013) physisorption and adsorption are preferred at low temperatures. Since a higher amount of CO₂ adsorbed is obtained at low temperature, it suggests that the process has a physical adsorption behavior. On the other hand, the increase of adsorption capacity occurs when the pressure is increased. The isotherms adsorption classification according to IUPAC show that, the figures above follows the isotherm-behavior of type-I that indicates a monolayer adsorption mechanism usually designated as microporous adsorbents materials (Sarker et al., 2017). The Langmuir model used for all samples are specified from equation 3 mentioned before.

Table 7. Langmuir parameters at different temperatures.

<i>T (K)</i>	<i>Langmuir coefficients</i>	Samples					
		<i>PAC</i>	<i>PACHP</i>	<i>PACSA</i>	<i>PACNA</i>	<i>PACNAU</i>	<i>PACNAUT</i>
313	<i>Q_m</i>	17.57	21.93	23.29	19.43	20.73	17.19
	<i>K_L</i>	0.373	0.462	0.926	0.527	0.378	0.314
	<i>R²</i>	0.9778	0.9697	0.9474	0.9665	0.9787	0.9821
343	<i>Q_m</i>	17.57	21.93	23.29	19.43	20.73	17.19
	<i>K_L</i>	0.207	0.221	0.423	0.274	0.188	0.176
	<i>R²</i>	0.9899	0.9886	0.9784	0.9865	0.9919	0.9923
373	<i>Q_m</i>	17.57	21.93	23.29	19.43	20.73	17.19
	<i>K_L</i>	0.126	0.119	0.219	0.159	0.105	0.108
	<i>R²</i>	0.9956	0.9959	0.9914	0.9935	0.997	0.9965

According to von Oepen et al., (1991), for being a small size molecule and having a higher quadrupole moment the CO₂ favors the adsorption at the time that enters in the activated carbon cavity. When the adsorbate and adsorbent interact, the change in standard enthalpy was caused by various forces, including van der Waals, hydrophobicity, hydrogen bonds, ligand exchange, dipole–dipole interactions and chemical bonds.

From table 7 it is clear to see in the ΔH (represented in table 7 as Q_m) values that CO₂ showed an interesting behavior. The Langmuir parameters shows that, the Q_m values are in the range of 17-23 kJ which mean that according to Zhou et al.,(2012) usually, the

amount of enthalpy changes (ΔH) for absolute physical adsorption is less than 20 kJ mol^{-1} , while for chemisorption it varies between 80 to 200 kJ mol^{-1} . There can also be observed a decrease in K_L values due to the increase in temperature, which confirms the adsorption exothermic nature. For all samples the R^2 are approximately to 1, which means that the correlation between the adsorption experimental data and Langmuir model are well fitted.

4.3. Comparison of different types of adsorbents for CO₂ adsorption

During past few years a lot of research to find better adsorbent for CO₂ adsorption has been made. These adsorbents have been treated chemically and thermally to increase their adsorption capacity. To know if the studied adsorbent has a good capacity for CO₂ adsorption it is important to make a comparison with some adsorbents previously studied. The table below shows the adsorption capacity of some adsorbents which have been activated chemically and thermally. As can be seen, all experiments were performed at pressure of 1 bar and the temperature ranged between 298 and 393 K. Comparing the other samples temperature with that one used in this work, it can be noted that exists a slightly difference between them. To be a good adsorbent for CO₂ adsorption, it can be observed from the results presented in the table 8 as well as mentioned before, the temperature interferes in CO₂ adsorption capacity as well as the type of activation, the adsorbents CO₂ content and the porosity size.

Here the only comparison that will be made is through the temperature of 373 K, considering the type of activation and the porosity size. For the A (1)-700 (char derived) adsorbent the activation was made with KOH and the porosity is microporous and the CO₂ adsorption capacity is $0,704 \text{ mmol g}^{-1}$ while for this work the type of activation was made with nitric acid, urea and thermally ($800 \text{ }^\circ\text{C}$) the porosity is micro/mesoporous size and CO₂ adsorption capacity is $0,6220 \text{ mmol g}^{-1}$ that was calculated by equation 1. The results of this work are much better than the rest of the adsorbents besides for the A (1)-700 (char derived) sample there is higher.

Table 8. Comparison of CO₂ adsorption capacity in the different types of adsorbents.

Adsorbents	Type of activation	Porosity	Pressure (bar)	Temperature (K)	Adsorption capacity(mmolg ⁻¹)	References
AHEP (Algae)	KOH activation	Micro/mesoporous	1	298	1,39	(Zhang et al., 2012)
				323	0,413	
A (1) -700 (char derived)	KOH activation	Microporous	1	348	0,211	(Olivares-Marín et al., 2011)
				298	3,136	
B (1) -700 (char derived)	KOH activation	Microporous	1	373	0,704	(Olivares-Marín et al., 2011)
				298	0,84	
C (1) – 700 (char derived)	KOH activation	Microporous	1	373	0,16	(Olivares-Marín et al., 2011)
				298	1,25	
GKOSN800 (Biomass Olive Stones)	CO ₂ & Heat Treatment	Micro/mesoporous	1	373	0,34	(Plaza et al., 2009)
				298	1,954	
P-C (polyethylene terephthalate)	KOH activation	Microporous	1	373	0,59	(A. Arenillas et al., 2005)
				303	1,09	
AC-MEA	MEA activation	Micro/mesoporous	1	343	0,273	(Mercedes Maroto-Valer et al., 2008)
				373	1,132	
				393	0,575	
HCM-DAH-1(Carbon Monoliths)	Amines	Meso/macroporous	1	298	0,125	(Olivares-marín et al., 2011)
32ACSH3	NaOH activation	Microporous	1	308	0,9295	(Bayhan and Kara, 2015)

Table 8. Comparison of CO₂ adsorption capacity in the different types of adsorbents

AAM-Silica	n/a	Micro/mesoporous	1	318	0,78	(Y. Zhao et al., 2012)
				333	0,58	
				348	0,49	
				363	0.43	
CB-FM	Magnetic fine particles	Micro/mesoporous	1	291	0,38	(Ammendola et al., 2017)
Empty fruit bunch AC	KOH activation	Microporous	1	298	2,634	(Parshetti et al., 2015)
				323	1,743	
				298	1,79	
Coconut AC	CO ₂ activation	Microporous	1	323	1,27	(Hao et al., 2011)
				373	0,43	
				298	1,88	
				323	1,29	
Norit SX2 (peat)	Steam activation	Mesoporous	1	373	0,61	(Rashidi et al., 2016)
				313	1,4721	
				343	0,8773	
PACNAUT (Modified Norit ROX 0.8)	Nitic acid, urea & thermally (800 0C)	Micro/mesoporous	1	373	0,622	This work

5. CONCLUSIONS

For being one of the biggest causes of greenhouse gases effects, CO₂ became a constant problem to the environment. Due to this, many researches to find the best technologies and processes have been developed for CO₂ capture. The cost of the process should be lower, for that the adsorption process is better considering, the knowledge of adsorbents is needed once through a known CO₂ adsorption capacity it can help with the size of equipment design.

The CO₂ adsorption experiments with a modified Norit ROX 0,8 activated carbon were performed using a total pressure range between 1 to 5 bar and the temperature at 313, 343 and 373 K to obtain the CO₂ adsorbed amount. Six activated carbon samples were examined by adsorption process. For these samples, the PAC sample is the main base and the PACSA, PACNA, PACHP, PACNAU and PACNAUT were activated through chemically and thermally treatments. Through the obtained data it can be concluded that between all the samples the PACNAUT has more capacity to capture CO₂, and on the other hand the PACSA was the one that has the lowest capacity for CO₂. The reason why we think that the PACNAUT has the higher CO₂ adsorption capacity is due to its high carbon content showed from the elemental analyses, and also from the high surface area showed from adsorption-desorption made with N₂ at 77 K which further fortifies the idea that the surface area is one of the main factors to obtain a large amount of carbon dioxide adsorption. The CO₂ adsorption isotherms obtained in this work follows a type-I isotherm according to the IUPAC classification, and represents a monolayer mechanism.

The study of adsorption isotherms of all these six samples allow us to see how much the temperature and pressure can affect the adsorption capacity. From these isotherms it is possible to observe that the PACNAUT adsorption results at 313 K and 5 bar the adsorption amount of CO₂ was 4,4537 mmol g⁻¹ while for 343 and 373 K the amount was 2,9805 and 2,1690 mmol g⁻¹ respectively. As can be seen the temperature really affects the CO₂ adsorption capacity since for best sample, we got the higher amount at 313 K, as we raise the temperature is visible that the CO₂ adsorption capacity decreases and this happens because when we rise the temperature and the van der Waals forces became weaker. We can complement saying that there is not much difference between the results obtained from 343 and 373 K, further reinforcing the idea that as we raise the temperature the CO₂ adsorption capacity decreases. It should be added that the pressure also affects

the adsorption once the CO₂ adsorption capacity increases as we increase the pressure. As mentioned before the experiments were carried out under temperature range between 313, 343 and 373 K and the pressure range between 1 to 5 bar. Based on this, we conclude that at low temperature and high pressure we can get high amount of CO₂. For future work we recommend for study the CO₂ adsorption capacity to keep the pressure and decrease the temperature lower than 313 K.

6. BIBLIOGRAPHY

- Ã, R.Q., Peterson, S., 2007. The energy – climate challenge : Recent trends in CO₂ emissions from fuel combustion 35, 5938–5952.
<https://doi.org/10.1016/j.enpol.2007.07.001>
- A, W.A., Ganvir, V.N., 2013. Preparation of Low Cost Activated Carbon from Tea Waste using Sulphuric Acid as Activating Agent Abstract : 2, 53–55.
- Ammendola, P., Raganati, F., Chirone, R., 2017. CO₂ adsorption on a fine activated carbon in a sound assisted fluidized bed: Thermodynamics and kinetics. Chem. Eng. J. 322, 302–313. <https://doi.org/10.1016/j.cej.2017.04.037>
- Arenillas, A., Rubiera, F., Parra, J.B., Ania, C.O., Pis, J.J., 2005. Surface modification of low cost carbons for their application in the environmental protection. Appl. Surf. Sci. 252, 619–624. <https://doi.org/10.1016/j.apsusc.2005.02.076>
- Arenillas, A., Smith, K.M., Drage, T.C., Snape, C.E., 2005. CO₂ capture using some fly ash-derived carbon materials 84, 2204–2210.
<https://doi.org/10.1016/j.fuel.2005.04.003>
- Audus, H., 1997. Greenhouse gas mitigation technology: An overview of the CO₂ capture and sequestration studies and further activities of the IEA Greenhouse Gas R&D Programme. Energy 22, 217–221. [https://doi.org/10.1016/S0360-5442\(96\)00107-7](https://doi.org/10.1016/S0360-5442(96)00107-7)
- Balsamo, M., Budinova, T., Erto, A., Lancia, A., Petrova, B., Petrov, N., Tsyntsarski, B., 2013. CO₂ adsorption onto synthetic activated carbon : Kinetic , thermodynamic and regeneration studies. Sep. Purif. Technol. 116, 214–221.
<https://doi.org/10.1016/j.seppur.2013.05.041>
- Bárcia, P.S., Bastin, L., Hurtado, E.J., Silva, J.A.C., Alírio, E., Chen, B., Bárcia, P.S., Bastin, L., Hurtado, E.J., Silva, J.A.C., Alírio, E., 2016. Single and Multicomponent Sorption of CO₂ , CH₄ and N₂ in a Microporous Metal-Organic Framework 6395. <https://doi.org/10.1080/01496390802282347>
- Barrett, E.P., Joyner, L.G., Halenda, P.P., 1951. The Determination of Pore Volume and Area Distributions in Porous Substances. I. Computations from Nitrogen Isotherms. J. Am. Chem. Soc. 73, 373–380. <https://doi.org/10.1021/ja01145a126>

- Bayhan, B., Kara, A., 2015. Length-weight and length-length relationships of the salemia *Sarpa SALPA* (Linnaeus, 1758) in Izmir Bay (Aegean Sea of Turkey). *Pak. J. Zool.* 47, 1141–1146. <https://doi.org/10.1016/j.energy.2014.09.079>
- Brunauer, S., Emmett, P.H., Teller, E., 1938. Adsorption of Gases in Multimolecular Layers. *J. Am. Chem. Soc.* 60, 309–319. <https://doi.org/10.1021/ja01269a023>
- Choi, J., Do, D.D., Do, H.D., 2001. Surface Diffusion of Adsorbed Molecules in Porous Media : Monolayer , Multilayer , and Capillary Condensation Regimes 4005–4031.
- Choi, S., Drese, J.H., Jones, C.W., 2009. Adsorbent materials for carbon dioxide capture from large anthropogenic point sources. *ChemSusChem* 2, 796–854. <https://doi.org/10.1002/cssc.200900036>
- Chung, Y., Na, B., Song, H.K., 1998. Short-cut evaluation of pressure swing adsorption systems 22, 637–640.
- Clarke, F.W., Irving Langmuir, B., 1916. Constitution of Solids and Liquids. *J. Am. Chem. Soc.* 38, 2221–2295. <https://doi.org/10.1021/ja02268a002>
- Continent, M., Asia, S., Nino-southern, E., Maritim, B., 2012. Climate Change and Variability over Malaysia : Gaps in Science and Research Information 41, 1355–1366.
- Damiani, D., Litynski, J.T., McIlvried, H.G., Vikara, D.M., Srivastava, R.D., 2012. The US Department of Energy’s R&D program to reduce greenhouse gas emissions through beneficial uses of carbon dioxide. *Greenh. Gases Sci. Technol.* 2, 9–19. <https://doi.org/10.1002/ghg>
- de Boer, J.H., Linsen, B.G., Osinga, T.J., 1965. Studies on pore systems in catalysts. VI. The universal t curve. *J. Catal.* 4, 643–648. [https://doi.org/10.1016/0021-9517\(65\)90263-0](https://doi.org/10.1016/0021-9517(65)90263-0)
- Do, D.D., 1998. Adsorption Analysis: Equilibria and Kinetics. <https://doi.org/10.1142/p111>
- Figuroa, D., Fout, T., Plasynski, S., Mcilvried, H., Srivastava, R.D., 2008. Advances in CO₂ capture technology — The U . S . Department of Energy ’ s Carbon Sequestration Program § 2, 9–20. [https://doi.org/10.1016/S1750-5836\(07\)00094-1](https://doi.org/10.1016/S1750-5836(07)00094-1)

- Guidance, U.T.H.E., 2011. ADSORPTION OF METHANE ON ACTIVATED CARBON BY VOLUMETRIC METHOD. National Institute Of Technology, Rourkela.
- Hamdan, M.E., Man, N., Shaffril, M., 2017. Farmers ' Adaptive Capacity towards the Impacts of Global Warming : A Review 9. <https://doi.org/10.5539/ass.v9n13p177>
- Ho, M.T., Allinson, G.W., Wiley, D.E., 2008. Reducing the Cost of CO₂ Capture from Flue Gases Using Pressure Swing Adsorption. *Ind. Eng. Chem. Res.* 47, 4883–4890. <https://doi.org/10.1021/ie070831e>
- Horvath, G., Kawazoe, K., 1983. Method for the calculation of effective pore size distribution in molecular sieve carbon. *J. Chem. Eng. Japan* 16, 470–475. <https://doi.org/10.1252/jcej.16.470>
- Hu, J., Liu, H., 2010. CO₂ Adsorption on Porous Materials.
- Ie, A., 2006. Energy technology perspectives scenarios and strategies to 2050: in support of the G8 Plan of Action.
- Iranshahi, D., Karimi, M., Amiri, S., Jafari, M., 2014. Modeling of naphtha reforming unit applying detailed description of kinetic in continuous. *Chem. Eng. Res. Des.* 1–24. <https://doi.org/10.1016/j.cherd.2013.12.012>
- Karimi, M., Rahimpour, M.R., Ra, R., Jafari, M., Iranshahi, D., Shariati, A., 2014. *Journal of Natural Gas Science and Engineering* Reducing environmental problems and increasing saving energy by proposing new configuration for moving bed thermally coupled reactors 17. <https://doi.org/10.1016/j.jngse.2014.01.007>
- Karimi, M., Rahimpour, M.R., Rafiei, R., Shariati, A., Iranshahi, D., 2015. Improving thermal efficiency and increasing production rate in the double technique Highlights : *Appl. Therm. Eng.* <https://doi.org/10.1016/j.applthermaleng.2015.10.109>
- Karimi, M., Silva, J.A.C., Gonçalves, C.N.P., Tuesta, J.L.D., Rodrigues, A.E., Gomes, H.T., 2018. CO₂ Capture in Chemically and Thermally Modified Activated Carbons Using Breakthrough Measurements : Experimental and Modeling Study. <https://doi.org/10.1021/acs.iecr.8b00953>
- Konduru, N., Lindner, P., Assaf-anid, N.M., 2007. Curbing the Greenhouse Effect by

- Carbon Dioxide Adsorption with Zeolite 13X 53, 3137–3143.
<https://doi.org/10.1002/aic>
- Lee, S., Park, S., 2015. Journal of Industrial and Engineering Chemistry A review on solid adsorbents for carbon dioxide capture. *J. Ind. Eng. Chem.* 23, 1–11.
<https://doi.org/10.1016/j.jiec.2014.09.001>
- Levan, M.D., Jakubczak, P., Lanuza, M., Galloway, D.B., Low, J.J., Willis, R.R., 2009. Screening of Metal - Organic Frameworks for Carbon Dioxide Capture from Flue Gas Using a Combined Experimental and Modeling Approach 18198–18199.
- Li, F., Fan, L., 2008. Clean coal conversion processes – progress and challenges 248–267. <https://doi.org/10.1039/b809218b>
- Li, J.R., Ma, Y., McCarthy, M.C., Sculley, J., Yu, J., Jeong, H.K., Balbuena, P.B., Zhou, H.C., 2011. Carbon dioxide capture-related gas adsorption and separation in metal-organic frameworks. *Coord. Chem. Rev.* 255, 1791–1823.
<https://doi.org/10.1016/j.ccr.2011.02.012>
- M. Ruthven, D., 1984. Principles of Adsorption and Adsorption Processes (1984, Wiley-Interscience).
- McDonald, J.D., Kracko, D., Doyle-eisele, M., Garner, C.E., Wegerski, C., Senft, A., Knipping, E., Shaw, S., Rohr, A., 2014. Carbon Capture and Sequestration: An Exploratory Inhalation Toxicity Assessment of Amine-Trapping Solvents and Their Degradation Products.
- Meisen, A., Shuai, X., 1997. Research and development issues in CO₂ capture. *Energy Convers. Manag.* 38, S37–S42. [https://doi.org/10.1016/S0196-8904\(96\)00242-7](https://doi.org/10.1016/S0196-8904(96)00242-7)
- Melikoglu, M., 2018. Current status and future of ocean energy sources : A global review. *Ocean Eng.* 148, 563–573. <https://doi.org/10.1016/j.oceaneng.2017.11.045>
- Mercedes Maroto-Valer, M., Lu, Z., Zhang, Y., Tang, Z., 2008. Sorbents for CO₂ capture from high carbon fly ashes. *Waste Manag.* 28, 2320–2328.
<https://doi.org/10.1016/j.wasman.2007.10.012>
- Mikhail, R.S., Brunauer, S., Bodor, E.E., 1968. Investigations of a complete pore structure analysis. I. Analysis of micropores. *J. Colloid Interface Sci.* 26, 45–53.
[https://doi.org/10.1016/0021-9797\(68\)90270-1](https://doi.org/10.1016/0021-9797(68)90270-1)

- Nurrokhmah, L., Abu-zahra, M.R.M., 2013. Evaluation of Handling and Reuse Approaches for the Waste Generated from MEA-based CO₂ Capture with the Consideration of Regulations in the UAE.
- Ochoa-ferna, E., 2006. Nanocrystalline Lithium Zirconate with Improved Kinetics for High-Temperature CO₂ Capture 1383–1385.
- Olivares-marín, M., García, S., Pevida, C., Wong, M.S., Maroto-valer, M., 2011. The influence of the precursor and synthesis method on the CO₂ capture capacity of carpet waste-based sorbents. *J. Environ. Manage.* 92, 2810–2817.
<https://doi.org/10.1016/j.jenvman.2011.06.031>
- Olivares-Marín, M., García, S., Pevida, C., Wong, M.S., Maroto-Valer, M., 2011. The influence of the precursor and synthesis method on the CO₂ capture capacity of carpet waste-based sorbents. *J. Environ. Manage.* 92, 2810–2817.
<https://doi.org/10.1016/j.jenvman.2011.06.031>
- Parshetti, G.K., Chowdhury, S., Balasubramanian, R., 2015. Biomass derived low-cost microporous adsorbents for efficient CO₂ capture. *Fuel* 148, 246–254.
<https://doi.org/10.1016/j.fuel.2015.01.032>
- Pérez-Marín, A.B., Zapata, V.M., Ortuño, J.F., Aguilar, M., Sáez, J., Lloréns, M., 2007. Removal of cadmium from aqueous solutions by adsorption onto orange waste. *J. Hazard. Mater.* 139, 122–131. <https://doi.org/10.1016/j.jhazmat.2006.06.008>
- Pevida, C., Drage, T.C., Snape, C.E., 2008. Silica-templated melamine – formaldehyde resin derived adsorbents for CO₂ capture 6.
<https://doi.org/10.1016/j.carbon.2008.06.026>
- Plaza, M.G., García, S., Rubiera, F., Pis, J.J., Pevida, C., 2010. Post-combustion CO₂ capture with a commercial activated carbon : Comparison of different regeneration strategies. *Chem. Eng. J.* 163, 41–47. <https://doi.org/10.1016/j.cej.2010.07.030>
- Plaza, M.G., Pevida, C., Arias, B., Feroso, J., Casal, M.D., Martín, C.F., Rubiera, F., Pis, J.J., 2009. Development of low-cost biomass-based adsorbents for postcombustion CO₂ capture. *Fuel* 88, 2442–2447.
<https://doi.org/10.1016/j.fuel.2009.02.025>
- Ramdin, M., 2015. CO₂ Capture with Ionic Liquids: Experiments and Molecular

Simulations. Delft University of Technology.

Rashidi, N.A., Yusup, S., Borhan, A., 2016. Isotherm and Thermodynamic Analysis of Carbon Dioxide on Activated Carbon. *Procedia Eng.* 148, 630–637.

<https://doi.org/10.1016/j.proeng.2016.06.527>

Rashidi, N.A., Yusup, S., Hameed, B.H., 2013. Kinetic studies on carbon dioxide capture using lignocellulosic based activated carbon. *Energy* 61, 440–446.

<https://doi.org/10.1016/j.energy.2013.08.050>

Rodríguez-Reinoso, F., 2002. Production and applications of activated carbons. *Handb. porous solids* 1766–1827.

Sarker, A.I., Aroonwilas, A., Veawab, A., 2017. Equilibrium and Kinetic Behaviour of CO₂ Adsorption onto Zeolites, Carbon Molecular Sieve and Activated Carbons.

Energy Procedia 114, 2450–2459. <https://doi.org/10.1016/j.egypro.2017.03.1394>

Shahkarami, S., 2017. CO₂ CAPTURE FROM GASES USING ACTIVATED CARBON. University of Saskatchewan Saskatoon By.

Silva, J.A.C., Cunha, A.F., Schumann, K., Rodrigues, A.E., 2014. Microporous and Mesoporous Materials Binary adsorption of CO₂ / CH₄ in binderless beads of 13X zeolite 187, 100–107.

<https://doi.org/10.1016/j.micromeso.2013.12.017>

Silva, J.A.C., Schumann, K., Rodrigues, A.E., 2012. Microporous and Mesoporous Materials Sorption and kinetics of CO₂ and CH₄ in binderless beads of 13X zeolite 158, 219–228.

<https://doi.org/10.1016/j.micromeso.2012.03.042>

Singh, V.K., Anil Kumar, E., 2016. Measurement and analysis of adsorption isotherms of CO₂ on activated carbon. *Appl. Therm. Eng.* 97, 77–86.

<https://doi.org/10.1016/j.applthermaleng.2015.10.052>

Singh, V.K., Kumar, E.A., 2017. Experimental investigation and thermodynamic analysis of CO₂ adsorption on activated carbons for cooling system. *J. CO₂ Util.*

17, 290–304. <https://doi.org/10.1016/j.jcou.2016.12.004>

Vieira, J.C., Soares, L.C., Froes-Silva, R.E.S., 2018. Comparing chemometric and Langmuir isotherm for determination of maximum capacity adsorption of arsenic by a biosorbent. *Microchem. J.* 137, 324–328.

<https://doi.org/10.1016/j.microc.2017.11.005>

- von Oepen, B., Kördel, W., Klein, W., 1991. Sorption of nonpolar and polar compounds to soils: Processes, measurements and experience with the applicability of the modified OECD-Guideline 106. *Chemosphere* 22, 285–304.
[https://doi.org/10.1016/0045-6535\(91\)90318-8](https://doi.org/10.1016/0045-6535(91)90318-8)
- Wahby, A., Ramos-fernandez, J.M., Martínez-escandell, M., Sepffillveda-, A., 2010. High-Surface-Area Carbon Molecular Sieves for Selective CO₂ Adsorption 974–981. <https://doi.org/10.1002/cssc.201000083>
- Wang, Q., Luo, J., Zhong, Z., Borgna, A., 2011. CO₂ capture by solid adsorbents and their applications: Current status and new trends. *Energy Environ. Sci.* 4, 42–55.
<https://doi.org/10.1039/c0ee00064g>
- Wang, Z., Mitch, W.A., 2015. Influence of Dissolved Metals on N-Nitrosamine Formation Under Amine-based CO₂ Capture Conditions Influence of Dissolved Metals on N- Nitrosamine Formation Under Amine-based CO₂ Capture Conditions Zimeng Wang and William A . Mitch. <https://doi.org/10.1021/acs.est.5b03085>
- Wennersten, R., Sun, Q., Li, H., 2014. The future potential for Carbon Capture and Storage in climate change mitigation e an overview from perspectives of technology , economy and risk. *J. Clean. Prod.* 1–13.
<https://doi.org/10.1016/j.jclepro.2014.09.023>
- Yang, Q., Lin, Y.S., 2006. Kinetics of Carbon Dioxide Sorption on Perovskite-Type Metal Oxides 6302–6310.
- Yu, C.H., Huang, C.H., Tan, C.S., 2012. A review of CO₂ capture by absorption and adsorption. *Aerosol Air Qual. Res.* 12, 745–769.
<https://doi.org/10.4209/aaqr.2012.05.0132>
- Zhang, Z., Wang, K., Atkinson, J.D., Yan, X., Li, X., Rood, M.J., Yan, Z., 2012. Sustainable and hierarchical porous Enteromorpha prolifera based carbon for CO₂ capture. *J. Hazard. Mater.* 229–230, 183–191.
<https://doi.org/10.1016/j.jhazmat.2012.05.094>
- Zhao, C., Chen, X., Zhao, C., 2012. K₂CO₃ / Al₂O₃ for Capturing CO₂ in Flue Gas from Power Plants . Part 1 : Carbonation Behaviors of K₂CO₃ / Al₂O₃ 1–5.
- Zhao, Y., Shen, Y., Bai, L., Ni, S., 2012. Carbon dioxide adsorption on polyacrylamide-

impregnated silica gel and breakthrough modeling. *Appl. Surf. Sci.* 261, 708–716.
<https://doi.org/10.1016/j.apsusc.2012.08.085>

Zhou, X., Yi, H., Tang, X., Deng, H., Liu, H., 2012. Thermodynamics for the adsorption of SO₂, NO and CO₂ from flue gas on activated carbon fiber. *Chem. Eng. J.* 200–202, 399–404. <https://doi.org/10.1016/j.cej.2012.06.013>

7. APPENDIX

7.1. Appendix A

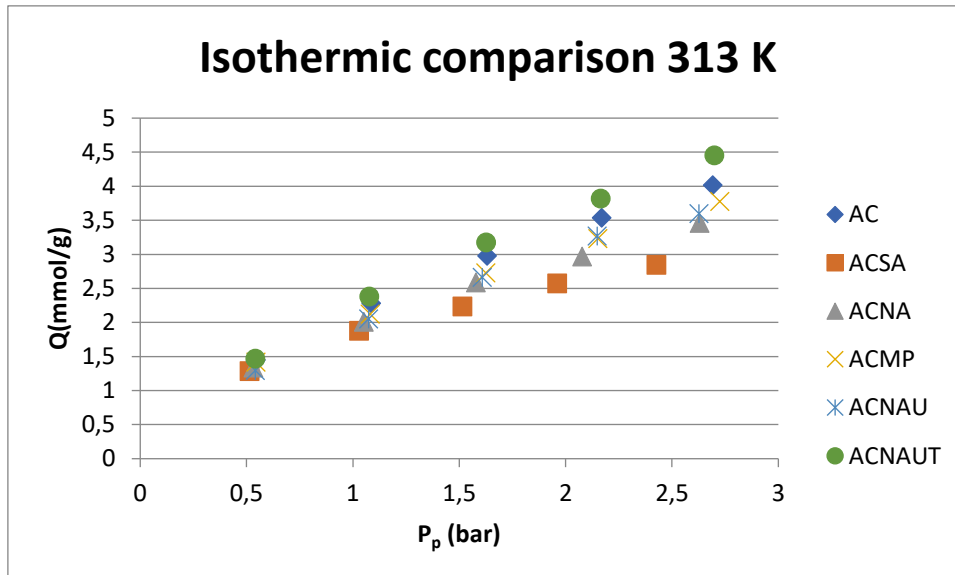


Figure 15. Comparison of CO₂ breakthrough adsorption measurement Isotherm of different activated carbon at 313 K

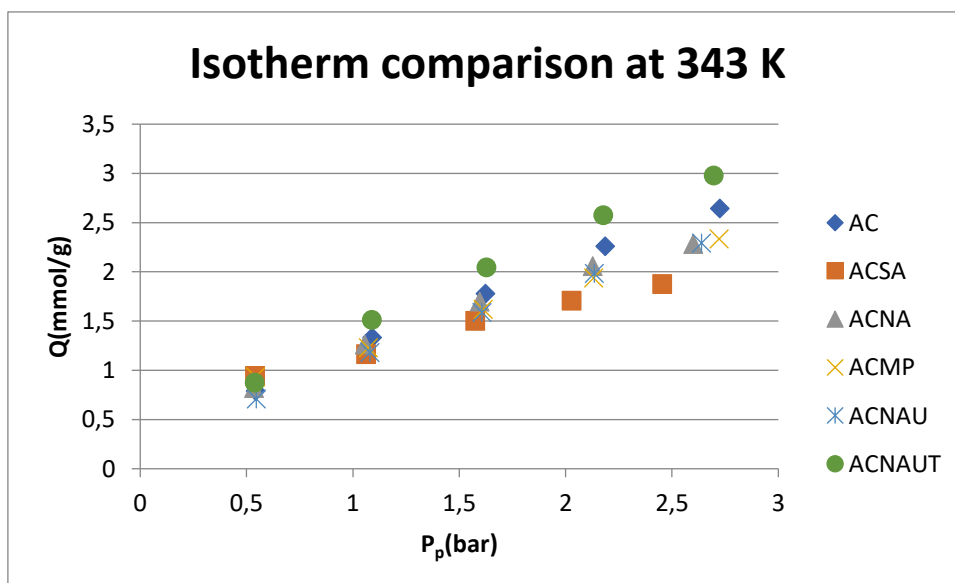


Figure 6. Comparison of CO₂ breakthrough adsorption measurement Isotherm of different activated carbon at 343 K

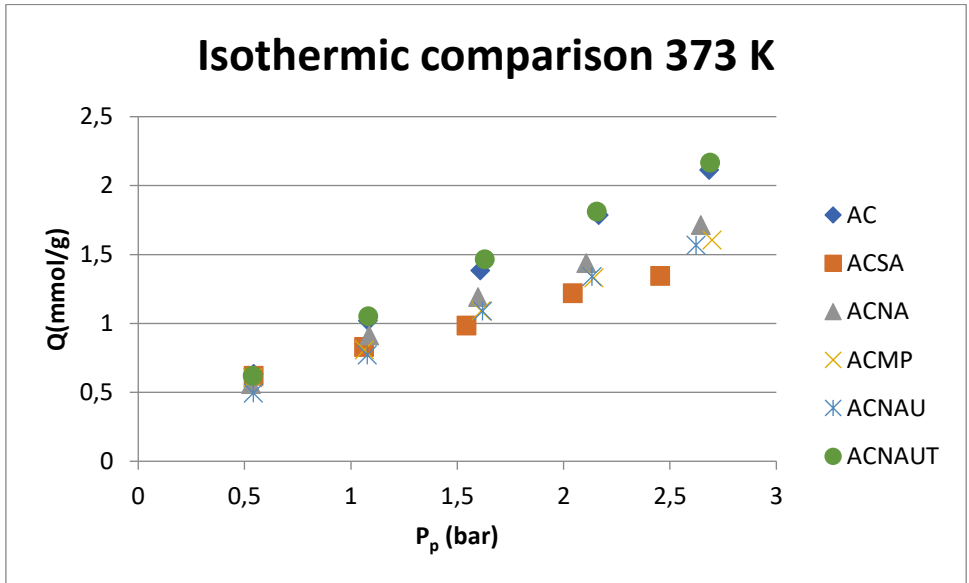


Figure 17. Comparison of CO₂ breakthrough adsorption measurement Isotherm of different activated carbon at 373 K

Table 9. Comparison of CO₂ breakthrough adsorption measurement Isotherm of different activated carbon at 313 K

AC		ACSA 313 K		ACNA	
Partial Pressure(bar)	Q(mmol/g)	Partial Pressure(bar)	Q(mmol/g)	Partial Pressure(bar)	Q(mmol/g)
0,544	1,450	0,514	1,289	0,532	1,341
1,086	2,282	1,029	1,880	1,051	2,010
1,631	2,977	1,514	2,235	1,578	2,589
2,170	3,538	1,961	2,574	2,077	2,967
2,692	4,016	2,426	2,845	2,630	3,461

Table 10. Comparison of CO₂ breakthrough adsorption measurement Isotherm of different activated carbon at 313 K

ACHP		ACNAU 313 K		ACNAUT	
Partial Pressure(bar)	Q(mmol/g)	Partial Pressure(bar)	Q(mmol/g)	Partial Pressure(bar)	Q(mmol/g)
0,543	1,419	0,541	1,295	0,541	1,472
1,081	2,124	1,074	2,051	1,077	2,381
1,625	2,730	1,609	2,662	1,626	3,176
2,150	3,234	2,148	3,269	2,164	3,820
2,725	3,778	2,627	3,598	2,699	4,453

Table 11. Comparison of CO₂ breakthrough adsorption measurement Isotherm of different activated carbon at 343 K

AC		ACSA 343 K		ACNA	
Partial Pressure(bar)	Q(mmol/g)	Partial Pressure(bar)	Q(mmol/g)	Partial Pressure(bar)	Q(mmol/g)
0,543	0,792	0,539	0,944	0,534	0,821
1,090	1,333	1,061	1,165	1,056	1,263
1,623	1,780	1,575	1,505	1,596	1,698
2,186	2,260	2,028	1,707	2,127	2,059
2,725	2,643	2,453	1,878	2,600	2,283

Table 12. Comparison of CO₂ breakthrough adsorption measurement Isotherm of different activated carbon at 343 K

ACHP		ACNAU 343 K		ACNAUT	
Partial Pressure(bar)	Q(mmol/g)	Partial Pressure(bar)	Q(mmol/g)	Partial Pressure(bar)	Q(mmol/g)
0,542	0,935	0,545	0,709	0,539	0,877
1,072	1,230	1,080	1,183	1,089	1,514
1,612	1,621	1,606	1,586	1,628	2,045
2,132	1,939	2,135	1,986	2,176	2,577
2,722	2,334	2,638	2,292	2,696	2,980

Table 13. Comparison of CO₂ breakthrough adsorption measurement Isotherm of different activated carbon at 373 K

AC		ACSA 373 K		ACNA	
Partial Pressure(bar)	Q(mmol/g)	Partial Pressure(bar)	Q(mmol/g)	Partial Pressure(bar)	Q(mmol/g)
0,543	0,792	0,539	0,944	0,534	0,821
1,090	1,333	1,061	1,165	1,056	1,263
1,623	1,780	1,575	1,505	1,596	1,698
2,186	2,260	2,028	1,707	2,127	2,059
2,725	2,643	2,453	1,878	2,600	2,283

Table 14. Comparison of CO₂ breakthrough adsorption measurement Isotherm of different activated carbon at 373 K

ACHP		ACNAU 373 K		ACNAUT	
Partial Pressure (bar)	Q(mmol/g)	Partial Pressure (bar)	Q(mmol/g)	Partial Pressure (bar)	Q(mmol/g)
0,542	0,935	0,545	0,709	0,539	0,877
1,072	1,230	1,080	1,183	1,089	1,514
1,612	1,621	1,606	1,586	1,628	2,045
2,132	1,939	2,135	1,986	2,176	2,577
2,722	2,334	2,638	2,292	2,696	2,980